AD NUMBER

AD819590

NEW LIMITATION CHANGE

TO

Approved for public release, distribution unlimited

FROM

Distribution authorized to U.S. Gov't. agencies and their contractors; Administrative/Operational Use; 21 Aug 1967. Other requests shall be referred to Air Force Technical Applications Center, Patrick, AFB, FL.

AUTHORITY

USAF ltr, 25 Jan 1972

RAYLEIGH WAVE SIGNAL TO NOISE ENHANCEMENT FOR A SMALL TELESEISM USING LASA, LRSM, AND OBSERVATORY STATIONS

21 August 1967

Prepared For

AIR FORCE TECHNICAL APPLICATIONS CENTER
Washington, D. C.

By

S. S. Alexander
THE PENNSYLVANIA STATE UNIVERSITY

D. B. Rabenstine
TELEDYNE, INC.

Under

Project VELA UNIFORM

Sponsored By

ADVANCED RESEARCH PROJECTS AGENCY
Nuclear Test Detection Office
ARPA Order No. 624

DISCLAIMER NOTICE

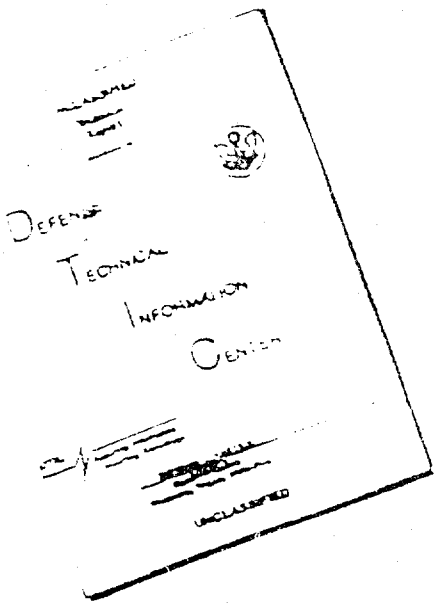

THIS DOCUMENT IS BEST QUALITY AVAILABLE. THE COPY FURNISHED TO DTIC CONTAINED A SIGNIFICANT NUMBER OF PAGES WHICH DO NOT REPRODUCE LEGIBLY.

RAYLEIGH WAVE SIGNAL TO NOISE ENHANCEMENT FOR A SMALL TELESEISM USING LASA, LRSM, AND OBSERVATORY STATIONS

SEISMIC DATA LABORATORY REPORT NO. 194

AFTAC Project No.:	VELA T/6702
Project Title:	Seismic Data Laboratory
ARPA Order No.:	624
ARPA Program Code No.:	5810
Name of Contractor:	TELEDYNE, INC.
Contract No.:	F 33657-67-C-1313
Date of Contract:	2 March 1967
Amount of Contract:	$ 1,736,617
Contract Expiration Date:	1 March 1968
Project Manager:	William C. Dean (703) 836-7644

P. O. Box 334, Alexandria, Virginia

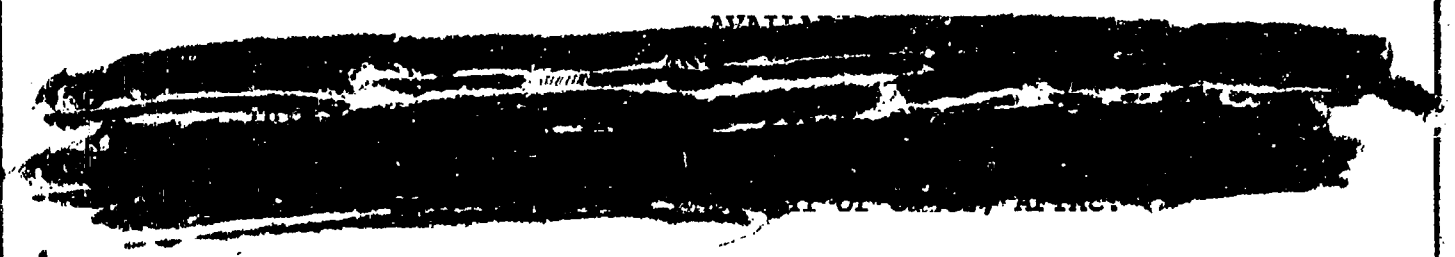

This research was supported by the Advanced Research Projects Agency, Nuclear Test Detection Office, under Project VELA-UNIFORM and accomplished under the technical direction of the Air Force Technical Applications Center under Contract F 33657-67-C-1313.

TABLE OF CONTENTS

	Page No.
ABSTRACT	
INTRODUCTION	1
METHODS OF ANALYSIS	3
A. Single Channel Methods	3
B. Multi-channel Methods	5
SIGNAL ENHANCEMENT CRITERIA	8
DATA PROCESSING	11
RESULTS	13
A. Comparison of Single Channel Enhancement Methods	13
B. Comparison of Multi-channel Enhancement Methods	15
CONCLUSIONS	23
RECOMMENDATIONS	25
REFERENCES	27
APPENDIX	
TABLES	
FIGURES	

TABLES

I. A. Epicenter Data

B. Distance-Azimuth Data for Greenland Sea Events

II. LASA Sensor Sub-Group Parameter Approximations

III. A. Observed S/N Values for LASA Stations

B. Observed S/N Values for LRSM Stations

IV. Signal to Noise Enhancement Summary (Array Methods 2 & 5)

LIST OF FIGURES

1. Configuration of the Large Aperture Seismic Array in Montana
2. LASA Long Period System "A" Response
3. Map showing locations of LRSM and Observatory Instruments used in this study.
4. LRSM Long Period System Response
5. Digital Band Pass Filter Response
6. Data Processing Flow Chart
7. Comparison of Several Signal Enhancement Procedures For A Single LASA Element
8. Comparison of Several Multichannel Signal Enhancement Procedures for 21 LASA LPZ Elements
9. Typical Multichannel Combinations of 5 LASA LPZ Elements Showing the Effect of Inter-Sensor Spacing
10. Typical Multichannel Combinations of 9 LASA LPZ Elements Showing the Effect of Inter-Sensor Spacing
11. Typical Results of Matched Filter Processing of LRSM (& VELA Observatory) LPZ Seismograms, & the Sum of 14 Such Matched Filter Outputs
12. Rayleigh Wave Enhancement vs. Number of Sensors with Inter-Sensor Spacing as a Parameter
13. Rayleigh Wave Enhancement vs. Inter-Sensor Spacing (N=5)
14. Rayleigh Wave Enhancement vs. Inter-Sensor Spacing (N=9)
15. Rayleigh Wave Enhancement vs. Aperture (N=5)
16. Rayleigh Wave Enhancement vs. Aperture (N=9)

ABSTRACT

Both single channel and array signal enhancement techniques have been applied to Rayleigh waves from a small Greenland Sea earthquake recorded at LASA and 13 LRSM or Observatory stations. Analysis of individual LASA long period recordings indicated that the matched filter increased S/N by more than 6 db over the mean S/N of band pass filtered (15-50 sec period) seismograms. Band pass filtering increased the mean S/N by only 1.5 db over the mean for unfiltered seismograms for LASA. Additional improvement in S/N from beam-forming both band passed and matched filtered traces approached the expected increase for uncorrelated noise provided the intersensor spacing (mesh-size) was at least 30 km. Comparable improvement was obtained for both single channel and beam-formed LRSM data. For LASA the beam-formed matched filter S/N for 13 stations was 17 db above the mean S/N for the individual band pass filtered seismograms; that for 13 LRSM stations was 15-16 db above the mean S/N of band pass filtered seismograms. Beam-forming matched filter seismograms consistently produced S/N values 7-9 db above the S/N for beam-formed band pass filtered seismograms. The effects of such array parameters as number of sensors, sensor spacing, and aperture on signal enhancement are evaluated for this event.

INTRODUCTION

The objective of this study is to compare the effectiveness of simple single channel and array methods for Rayleigh wave enhancement and to determine the dependence of these methods on array parameters such as number of sensors, sensor spacing, and aperture.

From the practical viewpoint it is important to know not only how well each available signal enhancement - noise reduction method performs, but also whether or not it can be used routinely on a large number of recordings. Only with this information is it possible to judge the "cost effectiveness" of a particular method for routine application. In this study we have attempted to evaluate and compare the simplest approaches or combinations thereof, for surface wave S/N (signal to noise ratio) improvement. These results then form a basis for future evaluation of more elaborate surface wave enhancement methods.

The most complicated approach we have included is array summing of the simple least squares matched filter seismograms, each of which is generated by the cross-correlation of a Z component trace with a known signal wave-form.

In addition we have investigated the influence of certain array parameters on the effectiveness of each method with a view toward eventually determining the relative merits of the LASA long period array versus the dispersed LRSM network for observing long period surface waves from small teleseismic events. The results presented in this context should be regarded as quite preliminary since they are based on the analysis of only one event.

The single channel methods applied to both LASA and LRSM

data were (1) the band pass filter, (2) the matched filter, and (3) a combined band pass, matched filter. The array methods applied to LASA were (1) phased sum of raw seismograms, (2) phased sum of band pass filtered seismograms, (3) phased sum of phase equalized seismograms, (4) phased sum of matched filter seismograms, (5) phased sum of combined band pass, matched filter seismograms and (6) matched filter of phased sum seismogram. For the LRSM array, only array methods (2), (4), and (5), above were applied. In the matched filter analysis, Rayleigh waves from a large, well-recorded event were used to search for the surface waves from a smaller event from the same region.

The data used in this study were recorded 18 November 1966, at the Montana LASA, LRSM stations, and other observatories by long period, vertical-component seismometers. The LASA station locations are shown in Figure 1. Each LASA sensor is located at a subarray center position, and each responds to seismic waves of various periods in a manner similar to that shown in Figure 2. Locations for the LRSM and Observatory instruments are shown in Figure 3, and their approximate response is illustrated in Figure 4. The epicenter and distance-azimuth data for the Greenland Sea events used are given in Table I.

In the following sections we outline in some detail the methods of analysis and procedures applied, present the salient results obtained for this event, summarize the important conclusions, and recommend several items deserving further investigation.

METHODS OF ANALYSIS

Several single-channel and multi-channel (array) methods were employed. All are characterized by their simplicity, straightforward practical application, and reasonable computer time requirements. In this section each method is presented, but approaches which are well-known and routine will not be developed.

Single Channel Methods

Band pass filter. Numerical band pass filtering is so commonplace that no development is needed here. In this study a non-recursive, phaseless filter (band pass 15-50 seconds period) was applied in the time domain. This filter response is shown in Figure 5.

Matched filter. The development of the matched filter approach in the time domain, and the justification of its application to the detection of surface waves from small events were given by Alexander and Rabenstine (Reference 1). Basically the technique amounts to searching a record $x(t)$ for a known waveform $y(t)$. It is assumed that $x(t) = ay(t) + n(t)$ where a is constant and $n(t)$ is a random process. The matched filter output is essentially a cross-correlation between $x(t)$ and $y(t)$.

In this particular application, $y(t)$ is the surface wave from a large event recorded at a given station. The time series $x(t)$ is a seismogram recorded at the same station and containing the surface wave from a much smaller event having as nearly as possible the same epicenter as the large event. The matched filter takes advantage of the fact that the two signals, having traveled essentially the same path will have

experienced the same phase distortion due to dispersion, so that cross-correlating them eliminates the propagation effects on phase, regardless of how complicated they may be.

The reason the matched filter is effective in enhancing dispersed surface waves is that it compresses the long, dispersed wave-train into a pulse of short duration, while random noise is not compressed. Thus, the energy density of the signal on the matched filter output compared to the energy density of the noise is increased; this amounts to an increase in S/N. The mathematical arguments which show this are presented in the Appendix.

Whereas the techniques derived and the results presented in the above referenced report were obtained operating in the time domain, identical results can be obtained at a considerable savings in computer time by operating in the frequency domain.

The matched filter output is given by

$$c_{xy}(t) = \int_{-\infty}^{\infty} X(\omega)\, Y^*(\omega) e^{i\omega t}\, d\omega \qquad (1)$$

where $X(\omega)$ = frequency spectrum of the test seismogram

$Y^*(\omega)$ = complex conjugate of the spectrum of the reference signal

Using the Cooley-Tukey method for fast Fourier transforms, implemented by McCowan (Reference 3), we transform $y(t)$ and $x(t)$, form the product $X(\omega)\, Y^*(\omega)$, and inverse transform to get the matched filter seismogram. In addition to speeding up the standard matched filter computations this approach has the advantage that (a) differences in instrument response can

be accounted for and any band pass filter or other shaping filters can be applied with negligible increase in computing time, (b) searching for a total of L reference signals in x(t) requires only L+1 Fourier transformations if the reference spectra are saved, and (c) the spectra are available for other uses such as measurement of radiation pattern as a function of frequency, Q measurements, phase velocity calculations, and excitation spectra as a function of magnitude.

Revised matched filter computer programs were written to implement this frequency domain approach.

The computation time is proportional to (MLogM) · K · L where M = sampling rate times the window length ($M \leq 4000$ in the present program) K= number of channels, L = number of regions or reference signals. For a sampling rate of 1 pt/sec and 21 channels the frequency domain matched filter would allow continuous search for a given reference waveform at about 6 pts/sec. This means that one could search 21 seismograms continuously for events from approximately six different source regions, using the CDC 1604B computer.

Combined band pass, matched filter. This was done in either of two equivalent ways:

a) first band pass filter the seismogram and then use this filtered seismogram as input for the matched filter.
b) do both in one pass through the frequency domain version of the matched program.

Multi-channel Methods

Phased sum of raw seismograms. The approach used in beamforming is so well-known that no elaboration is needed. Standard

beam-forming programs were used.

Phased sum of band pass filtered seismograms. The standard beam forming programs were applied to the band pass filtered seismograms.

Phased sum of phase equalized seismograms. A program was written to determine the transfer function for the LASA array, that is, the phase velocity as a function of frequency. The larger reference event from the Greenland Sea (Table 1) was used for this purpose, and all computations were carried out in the frequency domain. (The interpretation of the dispersion in terms of LASA structure is being carried out in a separate study, but the observed dispersion is all that is needed to phase equalize the seismogram to one element in the array). The equalization transforms the waveform at one station into an expected waveform at some reference station in the LASA array. The frequency domain matched filter program has an alternative option to perform the equalization on the smaller event using the observed phase velocity with frequency from the larger event.

Once each array element has been equalized the usual array summing is applied.

Phased sum of matched filter seismograms. The standard beam-forming programs were applied to the matched filter seismograms using the apparent velocity of the beginning of the reference signal window; this assures that the matched filter signal peaks will align.

Phased sum of combined band pass, matched filter seismograms.

The procedure here is the same as for item 4 above, except that the combined band pass, matched filter seismograms

are beam-formed. This results in signal enhancement due to the combination of (1) eliminating noise outside the signal band by band pass filtering (2) increasing the signal energy density relative to the noise energy density on each seismogram by the matched filter, and (3) $\sqrt{N}$ improvement in signal to noise by beam-forming.

Matched filter of phased sum of band pass filtered seismograms. In this approach the individual seismograms are first beam-formed and then match-filtered, using as a reference signal the phased sum of individual reference signals. It can be shown that this will produce less signal to noise enhancement than the phased sum of matched filter outputs unless the seismograms are phase equalized to a common station before summing in which case the results should be equivalent. However, over an array which does not strongly disperse the signals relative to one another, this method should be almost as good as phased summing matched filter outputs. It has the advantage that it takes only 1/N (N = number of sensors) as long to compute, since only one matched filter output must be obtained.

SIGNAL ENHANCEMENT CRITERIA

The question arises as to what measure of improvement in signal to noise is appropriate for dispersed surface waves. The problem is different from that for body waves in that the surface wave energy is progressively distributed over a longer time interval with increasing epicentral distance because of dispersion during propagation. This makes time domain measures of signal to noise such as ½ peak-to-peak amplitude divided by the RMS of the noise somewhat misleading and unrealistic. However, such a measure is acceptable for the matched filter output which is not dispersed.

In spite of the danger in using ½ (pk to pk)/RMS as an absolute measure of S/N, values of this S/N estimate before and after applying each method do provide a realistic measure of the improvement in S/N achieved. Therefore, we elected to adopt this as the standard definition of signal to noise throughout this study, namely

$$S/N = \tfrac{1}{2}\,(\text{peak-to-peak amplitude})\;(\text{RMS noise})^{-1} \qquad (2)$$

Partly this was done for convenience in that existing programs could be used, and partly to permit eventually the direct comparison of surface wave enhancement with long period body wave enhancement using array processing.

We chose the peak-to-peak amplitude of the Rayleigh waves by searching the seismogram for the extremum values over a time interval approximately corresponding to a group velocity window from 4 km/sec to 3 km/sec. For determining the matched filter peak-to-peak amplitude the search was made over on interval of 100 seconds centered on the expected signal

arrival time. Clearly this method breaks down when the signal level falls below the maximum noise peaks (≈ 3 x RMS). For this reason, some of our initial S/N estimates may be too large and thus the mean S/N against which we compare may be too large. This makes our estimates of improvement conservative.

It should be pointed out that because of the pulse-like shape of the matched filter signal (see Figure 7 for example), ½ of the peak-to-peak amplitude was consistently about 3 db smaller than the maximum positive signal amplitude. This suggests that for the matched filter S/N estimates it would be more appropriate to use the maximum signal amplitude in the future, or equivalently, increase the present S/N values by about 3 db. Thus, our estimates of S/N enhancement using the matched filter are always conservative.

In all cases the RMS estimates were made using at least a 30 minute interval immediately preceeding the Rayleigh wave arrival (4 km/sec). This interval, of course, includes the body wave phases, resulting perhaps in a slight increase in the RMS values obtained. This means that (a) our RMS values represent an upper bound on the true RMS of the winter noise at each station, (b) all S/N estimates calculated are conservative, and (c) comparisons of S/N improvement are still valid.

The measure of S/N improvement we adopted is given by the formula:

$$\text{S/N enhancement (db)} = 20 \text{ Log} \left[\frac{(S/N) \text{ on a sum trace)}}{\frac{1}{K} \sum_{i=1}^{K} (S/N)_i} \right] \quad (3)$$

K = number of elements used to form the sum trace

$(S/N)_i$ = signal to noise ratio on the i^{th} band pass filtered seismogram

Therefore, we are trying to improve on the mean of the K individual S/N values for band pass filtered data. In this study we found that the mean for various subsets of stations never deviated by more than 1 db from the mean S/N for all 21 LASA elements (4.1). These values are given in Table IV.

DATA PROCESSING

The flow chart shown in Figure 6 outlines the sequence of steps followed in processing the seismograms to obtain the desired outputs. LASA long period seismograms are recorded in multiplexed digital form at 800 bits-per-inch with a sampling rate of 5 points/second, whereas the LRSM and Observatory data are recorded in analog form on frequency-modulated tapes. In all cases the sampling rate of LASA seismograms has been reduced to 1 point/second, and the analog data have undergone A/D conversion and decimation to this same sampling rate. A standard sampling rate is required for both the matched filter and the array summing programs. Our choice of 1 point/second meets this requirement, keeps computer usage reasonable without sacrificing time resolution, and permits frequency analysis for all frequencies below .5 cps.

Surface waves from the events were sequentially recorded at the LASA on two multiplexed tapes. The first contained a part of the surface wave signature of the earlier event, and the second held not only the remaining data from the earlier event, but also the entire wave train from the later earthquake. Sampling rates on both tapes were reduced to 1 point/second, and the data were formated and merged onto a single library tape. The resulting tape was used to form two SUBSET tapes, one containing 60 minutes of data (Rayleigh minus 30 minutes to Rayleigh plus 30 minutes), and the other containing 10 minutes of the Rayleigh signature from the larger earthquake including data in the velocity window 4 to 3 km/sec. At this point we deviated from normal procedure to remove spikes caused by the tape merger mentioned earlier.

This was accomplished by a special program which used a straight line interpolation method to replace the spikes. As a result of these steps, we produced two LASA SUBSET tapes which were subsequently used as input to the matched filter, band pass filter, and summing programs.

The procedures applied to the LRSM and observatory data were essentially the same as those applied to the LASA data except for A/D conversion and deletion of tape merging.

RESULTS

In this section we present the major results obtained from the analysis of the small Greenland Sea event documented in Table I. All noise es imates given represent an upper bound on the RMS levels at each station since in most cases the noise sample intervals included the body waves. Values of S/N improvement obtained are to some extent systematically underestimated, (a) because estimated signal amplitudes before processing were too large for those stations where the maximum noise peak was above the maximum signal level and (b) because the matched filter signal estimate we use is always less than the maximum positive matched filter signal amplitude. Thus all the enhancement results we present may be regarded as conservative in assessing the usefulness of a particular approach.

Comparison of Single Channel Enhancement Methods

Band pass filter: The band pass filter appears to have been only marginally effective in reducing the overall noise level for LASA (see Table III and Figure 7). This implies only that there was little noise outside the signal frequency band. The mean of the RMS noise levels of the 21 LASA LPZ's was reduced only 1.5 db by band pass filtering with a pass band from 15 to 50 seconds (period). The generalization that this will always be the case should not be made. In many cases including the LRSM seismograms for this event, the noise field can be much stronger in 4-7 sec microseisms and/or above 50 sec microseisms, in which case band pass filtering will correspondingly be much more effective. For some of the LRSM stations band pass filtering led to noise reduction of as much as 11 db. However, the mean for all 13 stations was

reduced by 5.4 db.

Matched filter: The capability of the matched filter to compress the surface wave to a pulse, or band limited impulse, as described in the Appendix, proved to be a much more effective device for increasing the S/N ratio than band pass filtering (see Figure 7 and Table III). The mean S/N of the individual matched filter outputs for 21 LASA LPS's was 6.1 db higher than that of the band pass filtered surface waves. A similar improvement was obtained for most of the LRSM stations where the signal before matched filtering could be accurately measured above the noise (See Figure 11 and Table III).

Reliable estimates of S/N improvement could not be made for those channels where the signal was weak relative to the noise because the method for determining signal amplitude does not work when the signal is below the level of the largest noise peaks ($\approx$ 3 x RMS). However, visual examination of the matched filter output for these cases indicated that the signal was usually enhanced so that it stood out above the noise background. Thus, significant enhancement must have occurred in these cases as well. In synthetic cases Alexander and Rabenstine (Reference 1) show that typical teleseismic surface waves can be detected at a single station using the matched filter to levels of the order of S/N = .35 Therefore, for these low signal levels a different method must be devised for estimating S/N before matched filtering if reliable estimates of S/N are to be obtained.

When the S/N values before filtering are in error, then, they will be too large, so the estimates of S/N improvements which we obtained are conservative.

Band pass and matched filter: The mean S/N of the 21 LASA LPZ seismograms processed through both filters above was increased only a negligible amount (< 0.1 db) over that of the matched-filtered-only seismograms (see Figure 7 and Table III). This is as one would expect since the matched filter not only compresses the signal, but also acts as a band pass filter having a response given by the amplitude spectrum of the larger event (see Appendix). For the LRSM stations the mean S/N using both filters was about 1 db better than for the matched filter alone (see Table III).

Typical results comparing the effectiveness of all these single channel methods for LASA are shown in Figure 7. They are arranged in the order of increasing effectiveness with the matched filter results clearly the best, although there is little difference between the two matched filter cases. Figure 11 shows single channel matched filter results for 3 of the 13 LRSM stations; the top pair depicts the best, the middle set typical, and the third pair the poorest of the single channel results.

Comparison of Multi-Channel Enhancement Methods

A comparison of the different methods for the multi-channel cases is complicated by the fact that the effectiveness of each technique depends on a number of parameters, such as sensor spacing, array aperture, number of sensors, combining weights, etc., in addition to the character of the signal and noise on each channel. We shall discuss the various techniques making comments as to effects of some of these parameters.

In all cases Brennan weighting was used, i.e., (1) each

seismogram was normalized to unit noise power by dividing it by the RMS of a selected noise window within it, then (2) each seismogram was weighted by its S/N ratio. Brennan weighting emphasizes the better channels while de-emphasizing the noiser ones in all cases, such that the combined S/N is optimum and always greater than or equal to the best individual S/N value.

Phased sum of raw seismograms: The phased sum of raw (unfiltered), band pass filtered, and matched filter seismograms for LASA each gave a noise reduction approaching the square root of N (number of sensors) providing that the inter-sensor spacing used was greater than 30 km (see Figure 13) and 14). Spacings less than this include too much coherent noise to achieve $\sqrt{N}$ reduction. Spacings greater than 30 km do not seem to produce further noise reduction. Hartenberger (personal communication) has obtained similar results for LASA using a number of different noise intervals.

It is to be expected that as the array aperture is increased, the effects of dispersion will cause some signal loss in a simple summing process. However, in this experiment, using apertures up to the full diameter of LASA, this loss was not more than 2-3 db (see Figure 15 and 16). This is probably due mostly to the way in which signal was measured. Since the signals were shifted on a velocity very near that corresponding to the undispersed Airy phase, there was little change across LASA in Airy amplitudes, which was essentially our measure of signal amplitude. However, there was almost certainly some cancellation of signal energy at frequencies different from the Airy phase, which have varying velocities.

This can be seen by careful comparison of trace 1 with trace 3 in Figure 8.

Phased sum of band pass filtered seismograms: All of the above comments apply to this process as well. In addition, it was found that over LASA the S/N of these sums exceeded that of the unfiltered sums by more than ½ db in only one case, that being the array of 5 sensors with 10 km spacing. In all cases except this one, the noise outside the filter band was incoherent enough to be cancelled by the array combining just as well as by filtering. In the special case mentioned, the filtered sum was 1 db better in S/N than the unfiltered sum. Figure 8 shows the results for 21 LASA channels compared to results for the other methods. Figures 9 and 10 show similar comparisons for N = 5 and 9 respectively for inter-sensor spacings of 10 and 20 km.

The phased sums for different values of N(number of sensors) are shown by solid dots in Figure 12 with sensor spacing (mesh size) as a parameter. For example the combination A, B, (5 sensors) and A, B, C (9 sensors) correspond with an inter-sensor spacing of 10 km. Table II gives the parameter approximations for the sub-groups designated on the graph. While all the values fall below $\sqrt{N}$, if one connects points of equal mesh size (A,C to A,C,D for example) the slope is approximately the same as for $\sqrt{N}$; this suggests that although $\sqrt{N}$ is not achieved the percentage improvement on adding additional sensors keeping the inter-sensor spacing fixed is the same as for uncorrelated noise.

The S/N enhancements on beam-forming band pass filtered seismograms for various subsets of LASA stations in addition to all 21 are given in Table IV. Figures 13 and 14 show S/N

gain in db as a function of approximate inter-sensor spacing (mesh-size) for LASA using fixed values of N (number of sensors) of 5 and 9 respectively. In each instance uniform density of stations was maintained with inter-sensor spacing defined as the average mesh size. Also shown in these Figures is noise reduction on summing. It is clear that a mesh size of at least 30 km is required at LASA for achieving enhancement (noise reduction) near that expected for uncorrelated noise.

Sum of band pass filtered phase-equalized seismograms: The results with phase equalization of LASA seismograms were in all cases within ½ db of those obtained with simple phased sums of band pass filtered seismograms. This process should be expected to work much better than simple time shifting at large apertures, since phase equalization eliminates the effects of dispersion across the array. However, as mentioned above, this dispersion did not produce a significant signal change (by our definition of signal amplitude) for apertures up to 200 km, and thus it is to be expected that the phase equalization would not work much better than simple time shifting. This is evident from a comparison of trace 2 with trace 3 in Figure 8.

It might appear that phase equalization would be a convenient technique to eliminate the effects of dispersion across a very large (continental) array; however, there are several problems involved. Firstly, one needs a good phase velocity model for the entire region involved. Secondly, because of the azimuthal range involved, the only common point where the wave forms should match, and therefore to which one can equalize the phase, is the epicenter; and when one equalizes to the epicenter, one has essentially performed the matched filter

operation.

Phased sum of matched filter outputs. In summing the matched filter outputs one maintains the increase in signal level achieved in the matched filtering of the individual channels and adds to this any gains due to noise reduction in array combining.

The phased sums of matched filtered seismograms for different values of N (number of sensors) are shown by open circles in Figure 12 with sensor spacing (mesh size) as a parameter. As mentioned previously Table II gives the parameter approximations for the sub-groups designated on the graph. In each instance the matched filter sums are 7-9 db above the band pass filter sums for a given N and sub-set of sensors. The slope on connecting points of equal mesh size (AD to ADE for example)is approximately the same as for $\sqrt{N}$. Just as for the band pass results, this suggests that additional sensors,keeping the spacing fixed, gives the same percentage improvement in S/N as for uncorrelated noise.

The S/N enhancements on beam-forming matched filter seismograms are given in Table IV for various sub-sets of LASA stations. Figures 13 and 14 show the enhancement achieved by phase-summing LASA matched filter outputs compared to band pass filter phased sums for sub-sets of 5 and 9 sensors respectively as a function of the average inter-sensor spacing (mesh-size). In Figure 13 it is clear that for a given spacing the matched filter phased sum is 7-8 db above that for the band pass filtered phased sum (shown in the same Figures), with the 8 db values at the larger mesh sizes. For the 9 sensor case (Figure 14) the matched filter sums are from 8-9 db above the band pass filtered sum, again with the

larger differences at the larger spacings. Since the noise reduction values are very similar for both phased sums, the systematic increase in the difference with spacing and number of sensors probably is due to the fact that because of dispersion across LASA some signal is lost in phase-summing band pass filtered seismograms for more widely separated stations, while little is lost in phase summing matched filter seismograms. That is, aperture affects the phased-sum of band pass filtered seismograms more than it does the matched filtered sums. This is shown in Figures 15 and 16. Aperture over LASA has little effect on the combination of matched filter outputs since their undispersed, autocorrelation-like wave shapes coincide exactly as long as they are shifted properly. Only significant azimuthal differences in the source phase spectra between the reference event and the test event will result in matched filter signal cancellation on summing (see Appendix), whereas with the previous array sums, any azimuthal variation in the source phase spectrum will produce some signal cancellation on summing in addition to that due to dispersion across the array.

One might expect that errors in the epicenter location or origin time would cause difficulty in shifting the matched filter outputs. It can be shown, however, that if the seismograms from both events are time shifted on the same velocity, these errors tend to cancel out. In fact the positions of the maxima in the matched filter outputs can be used to estimate these errors.

The main problem involved in using the matched filter is the compilation of a library of master events to cover the

epicentral areas of interest.

Phased sum of band pass and matched filter seismograms. As was the result with the single channel seismograms, sums of LASA seismograms passed through both filters were identical to those of the matched-filter-only sums, within 0.5 db. Thus, all comments about matched filter sums are applicable here; and Figures 12,13,14 also represent this method for LASA; It can be concluded that in most cases, band pass filtering before matched filtering is unnecessary for LASA. For the LRSM stations the phased sum of the band pass matched filter seismograms was better by about 1.4 db than for matched-filter-only sums, so that band pass filtering the data would seem to be desirable for LRSM stations before matched filtering.

This method gave the best results of all the approaches we used. S/N values on beam-forming were consistently 7-9 db above the beam-formed band pass filtered S/N values as can be seen in Table IV. LRSM phased sums of matched filtered seismograms gave enhancements about the same as LASA. For 13 sensors S/N improvements over the mean of individual S/N values was 17 db for LASA compared to a value of 17.5 db expected for uncorrelated noise; for 13 LRSM stations the improvement was 15 (16) db over the mean of individual S/N values compared to a value of 15.5 (16.5) db expected for uncorrelated noise.

Matched filter of phased sum of band pass filtered seismograms. This was tried only for the LASA 9 sensor case with 30 km spacing; the resulting S/N was about 1-2 db lower than for phase summing individual matched filter seismograms. This

suggests that if this much loss in S/N by summing before matched filtering can be tolerated, this approach might be preferable because of the savings in computing time; this method takes only about $\frac{1}{N}$ (N = number of sensors) as long as match filtering individual channels and then phase summing. However, the reason this method worked as well as it did is because all of the signals were similar in waveform. As aperture increases and the dispersed signals become different in waveform this method should become progressively more inferior to the previous method. Also the weighting becomes a problem in applying this approach, since we do not have the individual S/N values for the matched filter seismograms; the Brennan weighting we used in the previous method can be shown to produce the optimum S/N enhancement if the noise is uncorrelated and stationary. Therefore, the combination of dissimilar waveforms and incorrect weighting may make this method less desirable. At this point, however, we have too little data on this approach to assess its merits fully.

Our results, then, indicate that of the methods investigated, phase-summing individual matched filter outputs produces the greatest enhancement in S/N and that in all types of phase summing of long period data, sensor spacings of at least 30 km are needed to assure that the noise in the 15-50 second period range is uncorrelated.

CONCLUSIONS

For a single Greenland Sea earthquake:

1. By means of a matched filter, the mean signal/ noise ratio for the surface wave on 21 LASA LPZ seismograms was increased 6 db over that of the band pass filtered seismograms. Mean S/N improvement of 3 to 4 db was obtained for 13 LRSM stations.

2. The signal/noise ratio of the matched filtered seismograms was independent of whether the seismograms were pre-filtered with a band pass filter for LASA. Pre-filtering LRSM seismograms produced matched filter results about 1.5 db better than not filtering.

3. An <u>additional</u> increase of signal/noise approaching $\sqrt{N}$ (N = number of sensors) was achieved by phased summing the matched filter outputs for LASA if an inter-sensor spacing of at least 30 km was maintained. A similar improvement was observed for the LRSM stations which had a still larger (but not uniform) spacing.

4. For array apertures as great as the full diameter of LASA, phased equalized summations showed little increase (< 1 db) in signal/noise over simple phased sums, both having been band pass filtered.

5. Phased sums of matched filter outputs were consistently 7-9 db above corresponding phased sums of band pass filtered seismograms.

6. A comparison of matched filter phased sums for 13 LASA and 13 LRSM stations (spacing $\geq$ 30 km) showed S/N gains of 17 and 15 (16) db respectively, over the mean of individual band pass filtered S/N values. In both cases this was within ½ db of the value expected for uncorrelated noise.

7. Aperture at LASA causes little or no signal loss for matched filter phased sums and only moderate signal loss (.5 to 3 db) on band pass filter phased sums for apertures up to 200 km. There was also little or no signal loss on phase summing the LRSM matched filter seismograms over a continental size aperture.

8. Even for the sensor spacings at which S/N gains were below those expected for uncorrelated noise, the percentage increase in S/N on adding additional sensors was approximately the same as for the uncorrelated case.

RECOMMENDATIONS

Several aspects of this study require further work and there are some follow-on areas of investigation which seem worthwhile. Specifically we recommend:

1. Additional small events be studied along the same lines as in the present study to confirm the findings of this study with regard to S/N gains and array parameters.

2. An attempt be made to define experimentally threshold signal detection levels for the matched filter method to verify the threshold values previously obtained in synthetic cases. To do this a new method for measuring initial S/N values must be developed.

3. Further work be done to assess the relative merits of matched filtering phased sum seismograms versus phase-summing individual matched filter seismograms.

4. Attempt to use both single channel and multi-channel matched filter approaches to obtain AR (ER) estimates for weak signals.

5. The empirical determination of scaling functions to adjust the matched filter reference spectrum to that appropriate for the event of interest.

6. Assessment of the "cost effectiveness" of the maximum likelihood matched filter approach (Reference 1) for LRSM and LASA surface waves. This will at the same time give additional information on the characteristics of long period noise at the various stations.

7. Further experimental work along the lines of Reference 1 and the Appendix of this report to obtain source parameters such as radiation pattern, initial phase, and excitation spectra for surface waves from small events.

8. An attempt be made to detect long period body waves by a matched filter approach where the reference signal consists of several body wave arrivals spanning a time interval long enough so that the noise in that interval is random and stationary.

REFERENCES

1. Alexander, S. S. and D. B. Rabenstine, "Detection of Surface Waves from Small Events at Teleseismic Distances", SDL Report No. 175, March 1967.

2. Aki, K., "Study of Earthquake Mechanism by a Method of Phase Equalization Applied to Rayleigh and Love Waves, J. Geophys. Res., Vol. 65, No. 2, 1960, pgs. 729-740.

3. McCowan, D. W., "Finite Fourier Transforms Theory and its Application to the Computation of Convolutions, Correlations, and Spectra," Tech. Memorandum No. 8-66, December 1966.

4. Papoulis, A., Probability, Random Variables and Stochastic Processes, McGraw-Hill Book Co., 1965.

APPENDIX

We present here a discussion of the details of the matched filter operation which shows that because the signal is compressed in time while the noise is not, S/N is increased.

The test seismogram x(t) has the Fourier representation

$$x(t) = \int_{-\infty}^{\infty} X(\omega)\, e^{i\omega t} d\omega \qquad \text{(A-1)}$$

and energy (by Parseval's identity)

$$E_x = \int_{-\infty}^{\infty} |X(\omega)|^2 \, d\omega \qquad \text{(A-2)}$$

The matched filter has the Fourier representation

$$c(t) = \int_{-\infty}^{\infty} X(\omega)\, Y^*(\omega)\, e^{i\omega t} d\omega \qquad \text{(A-3)}$$

where $Y^*(\omega)$ is the complex conjugate of the Fourier transform of the reference signal y(t), $(Y) = |Y(\omega)| e^{i\theta(\omega)}$). The associated energy of the matched filter output is

$$E_c = \int_{-\infty}^{\infty} |X(\omega)|^2 \, |Y(\omega)|^2 \, d\omega \qquad \text{(A-4)}$$

This is equivalent to the energy in x(t) after it is filtered with a function whose spectrum is $Y(\omega)$. Note that if we whiten $Y(\omega)$ (i.e. divide by $|Y(\omega)|$) so that instead of $Y^*(\omega)$ we have $Y^* / |Y(\omega)| = e^{-i\theta(\omega)}$ in equation (A-3), this equation becomes

$$cn(t) = \int_{-\infty}^{\infty} X(\omega) e^{-i[\theta(\omega) - \omega t]} \, d\omega \qquad \text{(A-5)}$$

with energy

$$E_{cn} = \int_{-\infty}^{\infty} |X(\omega)|^2 \, d\omega \qquad \text{(A-6)}$$

Thus, if the reference signal is whitened before applying it as a matched filter the energy of x(t) is conserved in the operation since $E_{cn} = E_x$.

What is left to show is that the signal is compressed in time while the noise is not.

If we take x(t) = s(t) + n(t) (signal + random noise), then,

$$X(\omega) = |S(\omega)| \exp\left[i\left(\varphi_{os}(\omega) - \frac{\omega\Delta}{C(\omega)} + \varphi_i(\omega)\right)\right]$$

$$+ |N(\omega)| \exp\left[i\left(\Psi(\omega) + \varphi_i(\omega)\right)\right] \qquad \text{(A-7)}$$

$$Y(\omega) = |Y(\omega)| \exp\left[-i\left(\varphi_{oy}(\omega) - \frac{\omega\Delta}{C(\omega)} + \varphi_i(\omega)\right)\right]$$

$$\equiv |Y(\omega| \; e^{-i\theta(\omega)} \qquad \text{(A-8)}$$

and

where

$\varphi_{os}(\omega)$ = phase spectrum at the source for s(t)

$\varphi_{oy}(\omega)$ = phase spectrum at the source for y(t)

$\varphi_i(\omega)$ = instrument phase spectrum (assumed identical for x and y)

$C(\omega)$ = phase velocity spectrum

Δ = epicentral distance

$|S(\omega)|$ = amplitude spectrum of s(t)

$|Y(\omega)|$ = amplitude spectrum of y(t)

$\theta(\omega)$ = total phase associated with y(t)

$\psi(\omega)$ = random phase associated with n(t)

Therefore,

$$XY^* = |S(\omega)|\ |Y(\omega)|\ \exp\left[i\left(\varphi_{os}(\omega) - \varphi_{oy}(\omega)\right)\right] + |N(\omega)|\ |Y(\omega)|\ \exp\left[i\left(\psi(\omega) - \theta(\omega)\right)\right] \quad \text{(A-9)}$$

The first term on the right hand side of the equation (A-9) is the matched filter signal spectrum and the second term is the noise spectrum. We will discuss each term separately. From the first term, the signal on the matched filter seismogram is given by

$$s_f(t) = \int_{-\infty}^{\infty} |S(\omega)|\ |Y(\omega)|\ \exp\left[i\left(\varphi_{os}(\omega) - \varphi_{oy}(\omega) + \omega t\right)\right] d\omega \quad \text{(A-10)}$$

If both s(t) and y(t) have the same phase spectrum at the source then $\varphi_{os} = \varphi_{oy}$ and (A-10) reduces to

$$s_f(t) = \int_{-\infty}^{\infty} |S(\omega)|\ |Y(\omega)| e^{i\omega t} d\omega \quad \text{(A-11)}$$

or for the whitened reference signal case

$$s_{fn}(t) = \int_{-\infty}^{\infty} |S(\omega)| e^{i\omega t} d\omega \quad \text{(A-12)}$$

We are now in a position to compare the energy density of $s_{fn}(t)$ with that of

$$s(t) = \int_{-\infty}^{\infty} |S(\omega)| \exp\left[i\left(\varphi_{os}(\omega) - \frac{\omega\Delta}{C(\omega)} + \varphi_i(\omega) + \omega t\right)\right] d\omega \qquad \text{(A-13)}$$

For $s_{fn}(t)$ the maximum energy density occurs at $t = 0$, since it is here that all the frequencies add together in phase (zero group delay for all frequencies) and

$$\int_{-\infty}^{\infty} |S(\omega)| d\omega \geq \int_{-\infty}^{\infty} |S(\omega)| e^{i\omega t} d\omega \text{ for all } t \neq 0.$$

For s(t) the energy is spread over a longer time window because the group delays (energy arrival times) are frequency-dependent; that is, the energy arrival at frequency ω occurs at a value of t such that

$$\frac{d}{d\omega}\left[\varphi_{os}(\omega) - \frac{\omega\Delta}{C(\omega)} + \varphi_i(\omega) + \omega t\right] = \varphi'_{os}(\omega) - \frac{\Delta}{U(\omega)} + \varphi'_i(\omega) + t = 0$$

or

$$t = \frac{\Delta}{U(\omega)} - \varphi'_{os}(\omega) - \varphi'_i(\omega) \qquad \text{(A-14)}$$

where

$U(\omega)$ = group velocity with frequency

$\varphi'_{os}(\omega)$ = group delay time at the source

$\varphi_i(\omega)$ = group delay time through the instrument

Since this total group delay time (A-14) is frequency dependent, energy at different frequencies arrives at different times on the seismogram. Given that the total energy of s(t) is equal to that of $s_{fn}(t)$ by the same arguments presented earlier, this means that the maximum energy density of s(t)

must always be less than that for $s_{fn}(t)$ (the case where the energy for every frequency arrives at the same time). Thus, the signal is compressed in time without loss of energy.

We now show how the noise is affected by the matched filter operation. What we compare is the noise

$$n(t) = \int_{-\infty}^{\infty} |N(\omega)| \exp\left[i\left(\psi(\omega) + \varphi_i(\omega) + \omega t\right)\right] d\omega \qquad \text{(A-15)}$$

with the matched filtered noise

$$n_f(t) = \int_{-\infty}^{\infty} N(\omega)\, Y^*(\omega) e^{i\omega t}\, d\omega \qquad \text{(A-16)}$$

or for the whitened reference signal case

$$n_{fn}(t) = \int_{-\infty}^{\infty} |N(\omega)| \exp\left[i\left(-\varphi_{oy}(\omega) + \frac{\omega\Delta}{C(\omega)} + \Psi(\omega) + \omega t\right)\right] d\omega \qquad \text{(A-17)}$$

The group delay at frequency ω in (A-17) is given by

$$t_d(\omega) = -\Psi'(\omega) - \frac{\Delta}{U(\omega)} + \varphi'_{oy}(\omega) \qquad \text{(A-18)}$$

Since $\Psi(\omega)$ is random, its derivatives $\Psi'(\omega)$ are also random. The second two terms on the left side of (A-18) introduce a systematic shift in group delay time with frequency, but because $\Psi'(\omega)$ is random, $t_d(\omega)$ is still random with the result that the noise is not compressed. Since the matched filter operating on $n(t)$ in the whitened, reference signal case conserves energy (by the earlier arguments) and is a linear filter with a flat amplitude spectrum, the noise has the same mean (zero) and the same variance (RMS amplitude) as before, so that the mean energy density in $n_{fn}(t)$ is the same as the mean energy density in $n(t)$.

(See Papoulis, 1965, pp.345-347 for a proof of this point. Stationarity is assumed).

Thus, we conclude that the matched filter operation increases the signal energy density while not increasing the noise energy density. This means an enhancement in any conventional time domain S/N estimate.

Since the case where the reference signal spectrum of the matched filter is not whitened (the usual case) is equivalent to prefiltering x(t) with a phaseless filter whose spectrum is $|Y(\omega)|$ and then using the whitened reference signal, all the arguments above with respect to increasing signal energy density relative to the noise energy density hold for this case as well.

Since $|S(\omega)|$ is not identical to $|Y(\omega)|$ in practice, one should shape $|Y(\omega)|$ so that it duplicates $|S(\omega)|$ as nearly as possible. This filter $|Z(\omega)|$ $|Y(\omega)| \cong |S(\omega)|$ has the effect of emphasizing the frequencies where signal is present and de-emphasizing the frequency ranges where signal is low. As yet, we do not have empirical shaping functions $|Z(\omega)|$ as a function of body wave magnitude, so for the present we simply use $|Y(\omega)|$. Apparently $|Y(\omega)|$ is a reasonable first approximation for $|S(\omega)|$, because the matched filter results for this case are better than for the whitened case in the tests we have made thus far.

As a final note it should be pointed out that all the analysis done in this Appendix assumes infinite limits in both time and frequency, while in practice we work with finite times and finite frequency bands. However, it can easily be shown that the results of this section apply equally well to the actual situations involving finite intervals.

Table 1-A Epicenter Data*

Date	Area	Latitude	Origin Time (GMT)	Depth (km)	Longitude	Magnitude
18 Nov.66	Greenland Sea	73.4 N	18:07:54.0	33.	6.8 E	4.6
18 Nov.66	Greenland Sea	73.4 N	18:48:43.9	33.	6.8 E	4.9

*USC&GS

Table 1-B Distance-Azimuth Data for Greenland Sea Events

STATION	DISTANCE (km)	AZIMUTH	BACK-AZIMUTH
LASA (center)	5768.9	306.4	19.7
SV3QB	3791.5	277.9	29.46
HN-ME	4690.3	272.7	24.4
RK-ON	5000.3	298.1	23.6
PG-BC	5368.8	322.2	17.3
BMO	6232.3	314.8	16.7
MO-ID	6397.6	313.3	16.6
UBO	6525.8	306.7	17.5
AX2AL	6644.8	283.1	19.4
EU2AL	6697.2	284.7	19.3
WMO	6816.8	295.1	18.4
BE-FL	6922.4	277.9	18.9
JE-LA	6929.9	288.1	18.7
MN-NV	6936.5	313.4	15.4

Table II.

LASA Sensor Sub-Group Parameter Approximations

N	Sensors	Approximate Spacing (km)	Approximate Aperture (km)
5	A0, B1-4	10	18
5	A0, C1-4	15	30
5	C2-4, D2-3	20	38
5	A0, D1-4	30	56
5	A0, E1-4	60	116
5	A0, F1-4	100	200
9	A0, B1-4, C1-4	10	30
9	A0, C1-4, D1-4	15	56
9	A0, D1-4, E1-4	30	116
9	A0, E1-4, F1-4	60	200
13	A0, D1-4, E1-4, F1-4	--	200
21	ALL	--	200

Table III-A.

Observed S/N Values for LASA Stations

STATION	S/N Raw Seismograms	S/N Band Pass Filtered Seismograms	S/N Matched Filter on Raw Seismograms	S/N Matched Filter on Band Pass Filtered Seismograms
B1	3.1	3.4	8.3	8.6
F3	3.8	4.7	10.2	10.3
F4	3.3	4.5	8.5	8.7
AO	3.6	3.9	9.0	9.0
B3	4.3	4.4	9.1	9.0
C4	3.4	4.1	9.2	9.4
B4	3.2	3.8	7.9	7.8
C1	4.0	3.5	7.7	7.6
C2	4.1	4.4	9.7	9.7
B2	4.6	4.5	9.1	9.1
C3	4.7	4.7	8.7	8.7
D3	3.7	4.0	9.0	9.0
D4	4.3	4.6	7.0	7.1
D1	3.7	4.4	10.5	10.3
D2	4.9	6.0	11.0	11.0
E3	4.3	4.6	8.4	8.5
E4	4.6	4.4	9.4	9.4
E1	3.7	3.3	4.7	4.6
F1	3.3	3.3	6.4	7.0
E2	2.6	2.6	4.9	5.0
F2	3.3	2.9	5.4	5.7

Table III-B.

Observed S/N Values for LRSM Stations

STATION	S/N Raw Seismograms	S/N Band Pass Filtered Seismograms	S/N Matched Filter on Raw Seismograms	S/N Matched Filter on Band Pass Filtered Seismograms
SV3QB	2.4*	3.2*	1.9	2.1
HN-ME	3.0*	3.4*	1.8	2.3
RK-ON	7.5	9.6	14.3	14.7
PG-BC	8.9	16.3	17.1	17.3
KC-MO	6.4	6.9	9.2	8.8
BMO	4.4*	3.7	7.8	9.3
MO-ID	6.1	6.9	10.5	10.2
UBO	6.5*	3.9	4.5	7.7
AX2AL	3.1	6.7	10.0	10.4
EU2AL	1.8	3.9	5.7	6.2
WMO	6.3	8.6	15.4	15.2
BE-FL	3.4*	3.5*	2.2	2.6
JE-LA	2.0*	4.6*	1.0	4.5
MN-MV	3.3*	3.8*	2.2	2.2

* Noise Peak Mistaken For Signal by Computer

Table IV

Signal to Noise Enhancement Summary (Array Methods 2 & 5)

		BAND PASS FILTER							MATCHED FILTER (& B.P. Filter)							
	N	$\bar{a}\sqrt{N} \cdot \bar{a}$	$\left[\sum_{n=1}^{N} a_n^2\right]^{\frac{1}{2}}$	a_{sum}	NR (db)	SNG (db)	PRED SNG (db)		$\bar{a}\sqrt{N} \cdot \bar{a}$	$\left[\sum_{1}^{N} a_k^2\right]^{\frac{1}{2}}$	a_{sum}	NR (db)	SNG (db)	PRED SNG (db)	OVERALL SNG (db)	
LRSM	13	6.0* (5.2)	21.7	25.3	22.9	12.1	11.6	12.5	8.1	29.2	34.4	32.9	12.6	12.2	12.6	14.8 (16)
LASA ALL	21	4.1	18.8	19.1	10.0	9.8	7.7	13.4	8.4	38.5	39.0	23.4	9.1	8.9	13.4	15.2
A,D,E,F	13	4.1	14.8	15.1	10.7	11.4	8.3	11.3	8.1	29.2	30.2	28.7	11.2	11.0	11.4	16.9
A,E,F	9	3.8	11.4	11.6	9.0	11.1	7.5	9.6	7.6	22.8	23.5	26.0	10.9	10.7	9.8	16.7
A,D,E	9	4.2	12.6	12.8	9.6	9.2	7.2	9.7	8.2	24.6	25.4	24.7	9.7	9.5	9.8	15.4
A,C,D	9	4.4	13.2	13.3	8.4	7.0	5.7	9.6	9.1	27.3	27.4	18.8	6.4	6.3	9.6	12.6
A,B,C	9	4.1	12.3	12.3	6.0	4.0	3.3	9.6	8.8	26.4	26.4	13.6	3.9	3.8	9.6	10.4
A,F	5	3.9	8.7	8.7	6.2	6.3	4.1	7.1	8.1	18.1	18.5	15.6	5.7	5.7	7.1	12.0
A,E	5	3.7	8.3	8.5	7.0	7.7	5.4	7.1	7.3	16.3	17.0	18.4	8.1	8.0	7.3	13.9
A,D	5	4.6	10.3	10.3	8.2	7.1	5.1	7.1	9.3	20.8	21.0	19.0	6.4	6.2	7.1	12.3
C2,3,4,D2,3,5	5	4.7	10.5	10.5	8.4	6.1	5.2	7.1	9.5	21.2	21.4	18.0	5.5	5.5	7.0	11.7
A,C	5	4.1	9.2	9.2	6.4	4.4	3.9	7.0	8.9	19.9	19.9	14.4	4.2	4.2	7.0	10.9
A,B	5	4.0	8.9	9.0	5.0	2.6	1.9	7.0	8.7	19.4	19.5	11.7	2.6	2.5	7.0	9.3

a_n = S/N on nth element

$\bar{a}$ = Mean S/N over N elements

a_{sum} = S/N on sum trace

NR = Noise reduction

SNG = S/N Gain

PRED SNG = Predicted S/N Gain

*This value is too large due to noise being taken for signal. The value in parenthesis has been corrected to account approximately for this source of error.

Table IV

Signal to Noise Enhancement Summary (Array Methods 2 & 5)

		BAND PASS FILTER							MATCHED FILTER (& B.P. Filter)							
	N	$\bar{a}$	$\sqrt{N}\cdot\bar{a}$	$\left[\sum_{n=1}^{N} a_n^2\right]^{\frac{1}{2}}$	a_{sum}	$NR_{(db)}$	$SNG_{(db)}$	$PRED\ SNG_{(db)}$	$\bar{a}\sqrt{N}\cdot\bar{a}$	$\left[\sum_{1}^{N} a_k^2\right]^{\frac{1}{2}}$	a_{sum}	$NR_{(db)}$	$SNG_{(db)}$	$PPED\ SNG_{(db)}$	$OVERALL\ SNG_{(db)}$
LRSM	13	6.0* (5.2)	21.7	25.3	22.9	12.1	11.6	12.5	8.1	29.2	34.4	32.9	12.6	12.2	12.6	14.8 (16)
LASA ALL	21	4.1	18.8	19.1	10.0	9.8	7.7	13.4	8.4	38.5	39.0	23.4	9.1	8.9	13.4	15.2
A,D,E,F	13	4.1	14.8	15.1	10.7	11.4	8.3	11.3	8.1	29.2	30.2	28.7	11.2	11.0	11.4	16.9
A,E,F	9	3.8	11.4	11.6	9.0	11.1	7.5	9.6	7.6	22.8	23.5	26.0	10.9	10.7	9.8	16.7
A,D,E	9	4.2	12.6	12.8	9.6	9.2	7.2	9.7	8.2	24.6	25.4	24.7	9.7	9.5	9.8	15.4
A,C,D	9	4.4	13.2	13.3	8.4	7.0	5.7	9.6	9.1	27.3	27.4	18.8	6.4	6.3	9.6	12.6
A,B,C	9	4.1	12.3	12.3	8.0	4.0	3.3	9.6	8.8	26.4	26.4	13.6	3.9	3.8	9.6	10.4
B,F	5	3.9	8.7	8.7	6.2	6.3	4.1	7.1	8.1	18.1	18.5	15.6	5.7	5.7	7.1	12.0
A,E	5	3.7	8.3	8.5	7.0	7.7	5.4	7.1	7.3	16.3	17.0	18.4	8.1	8.0	7.3	13.9
A,D	5	4.6	10.3	10.3	8.2	7.1	5.1	7.1	9.3	20.8	21.0	19.0	6.4	6.2	7.1	12.3
C2,3,4,D2,3,5	5	4.7	10.5	10.5	8.4	6.1	5.2	7.1	9.5	21.2	21.4	18.0	5.5	5.5	7.0	11.7
A,C	5	4.1	9.2	9.2	6.4	4.4	3.9	7.0	8.9	19.9	19.9	14.4	4.2	4.2	7.0	10.9
A,B	5	4.0	8.9	9.0	5.0	2.6	1.9	7.0	8.7	19.4	19.5	11.7	2.6	2.5	7.0	9.3

a_n = S/N on nth element

$\bar{a}$ = Mean S/N over N elements

a_{sum} = S/N on sum trace

NR = Noise reduction

SNG = S/N Gain

PRED
SNG = Predicted S/N Gain

*This value is too large due to noise being taken for signal. The value in parenthesis has been corrected to account approximately for this source of error.

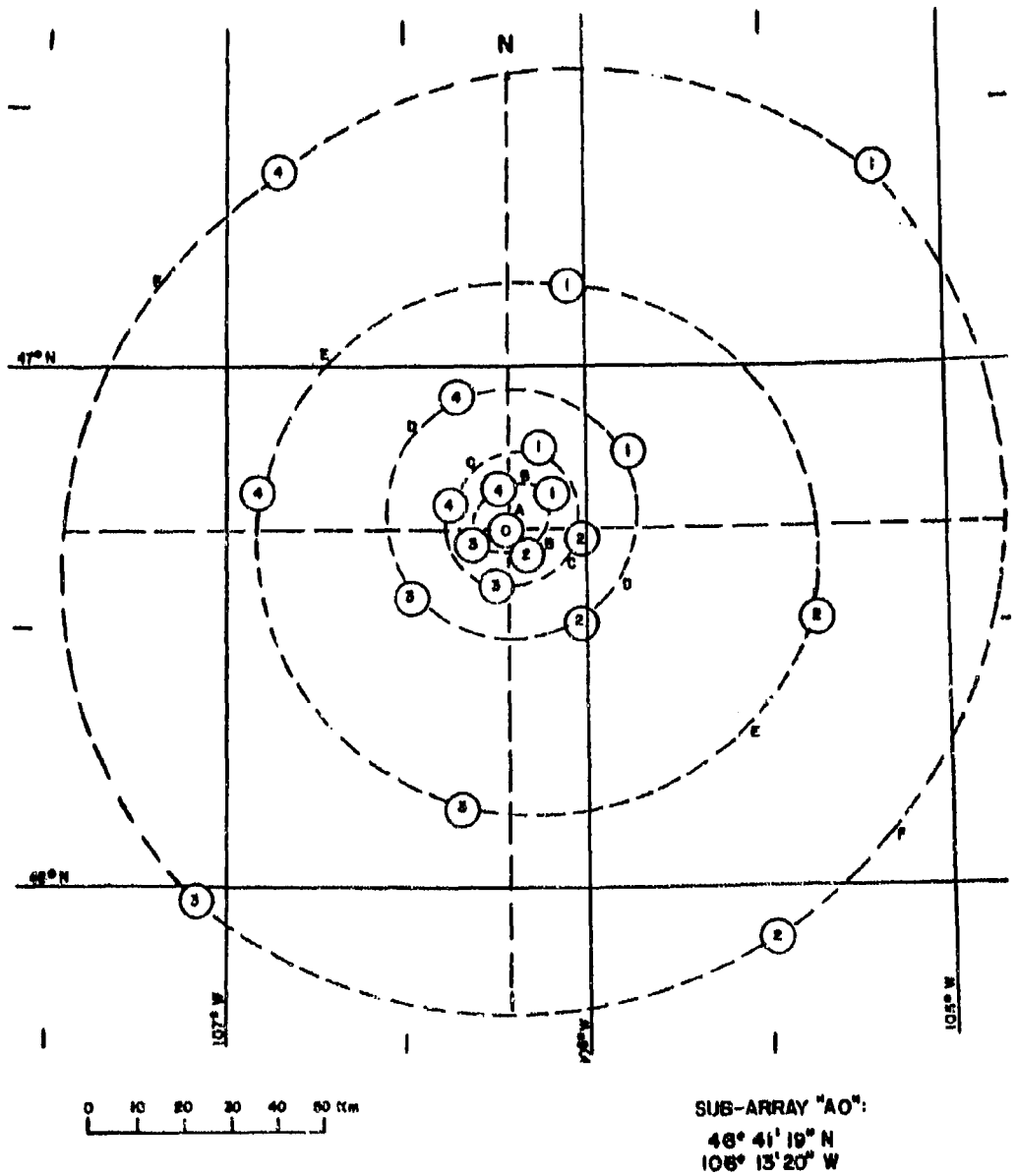

Figure 1. Configuration of the Large Aperture Seismic Array in Montana

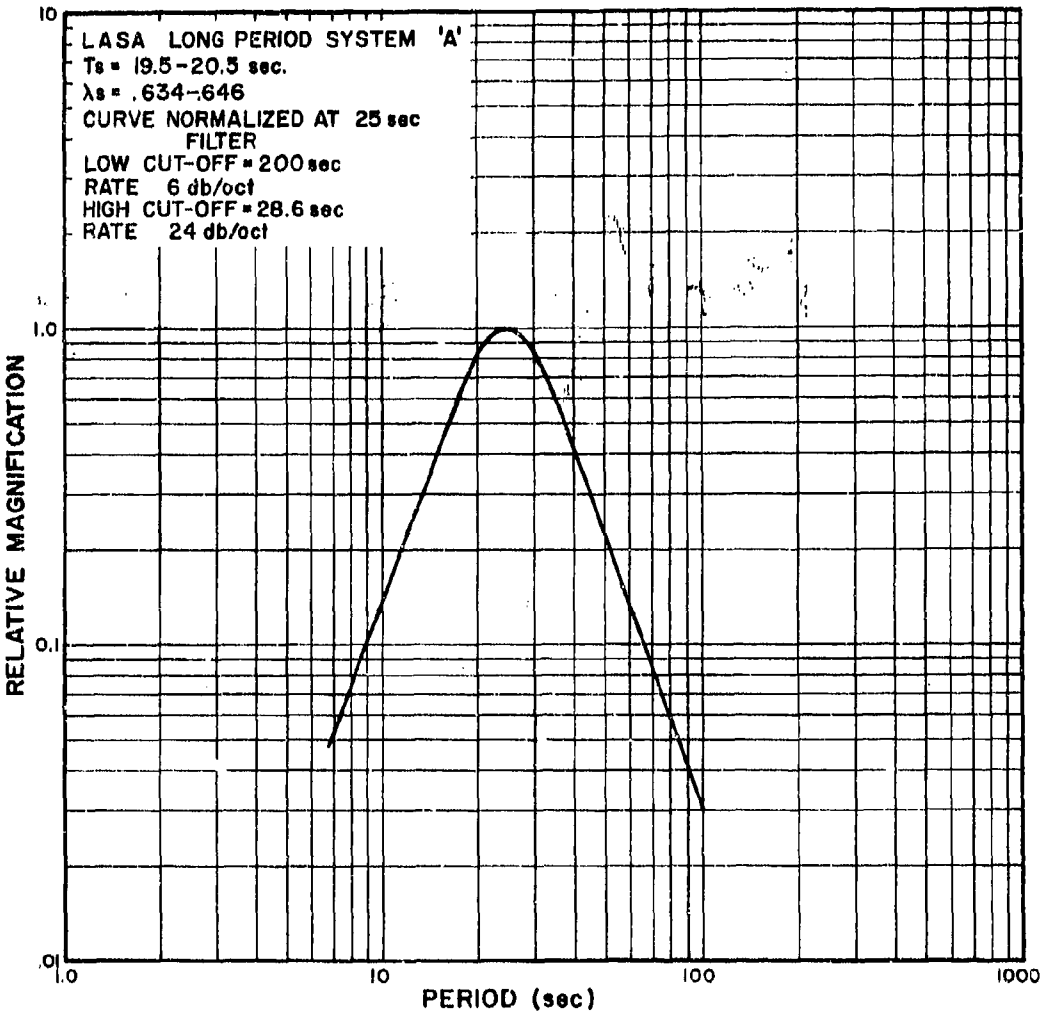

Figure 2. LASA Long Period System "A" Response

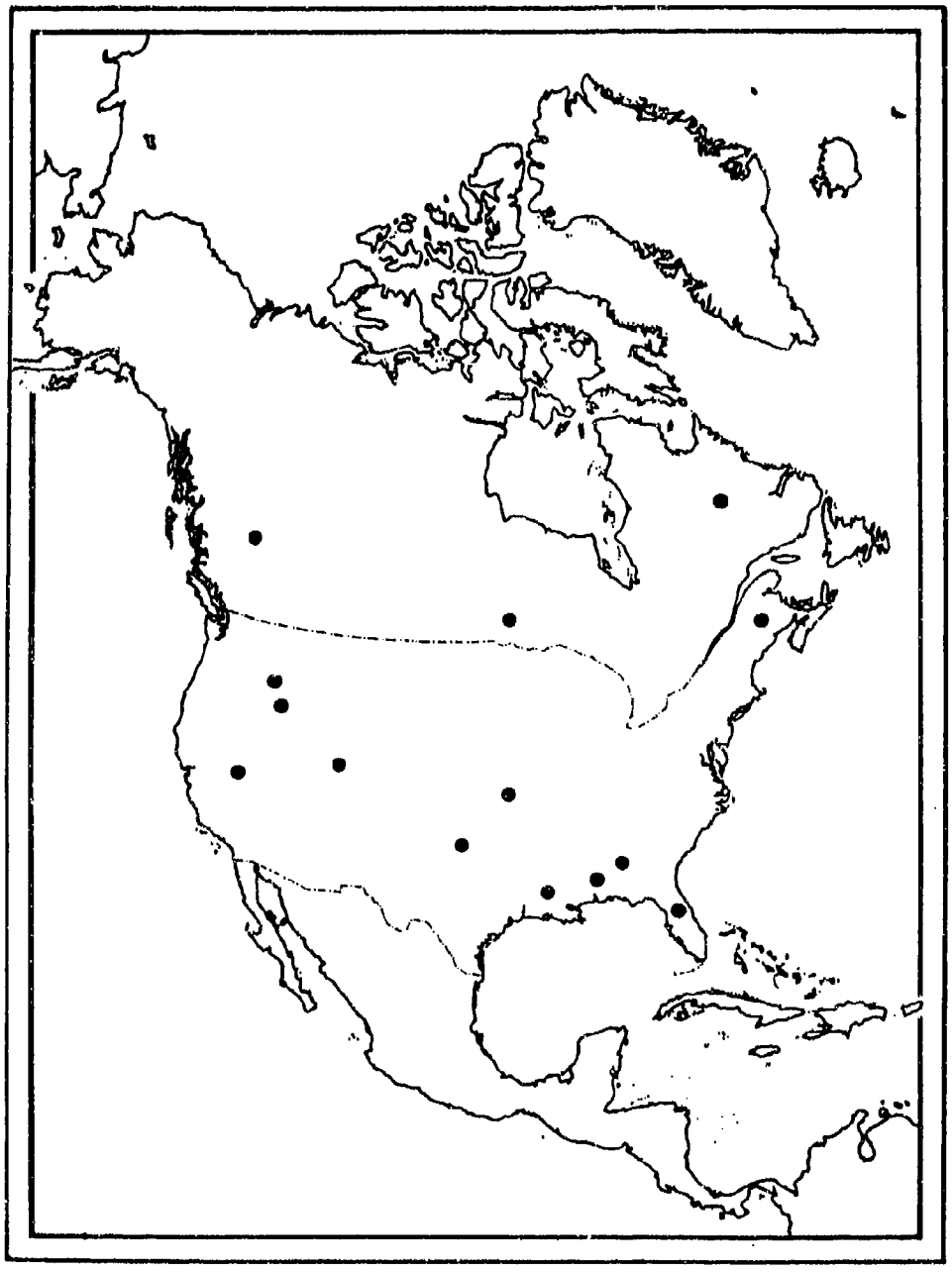

Figure 3. Map Showing Locations of LRSM and Observatory Instruments Used in this Study

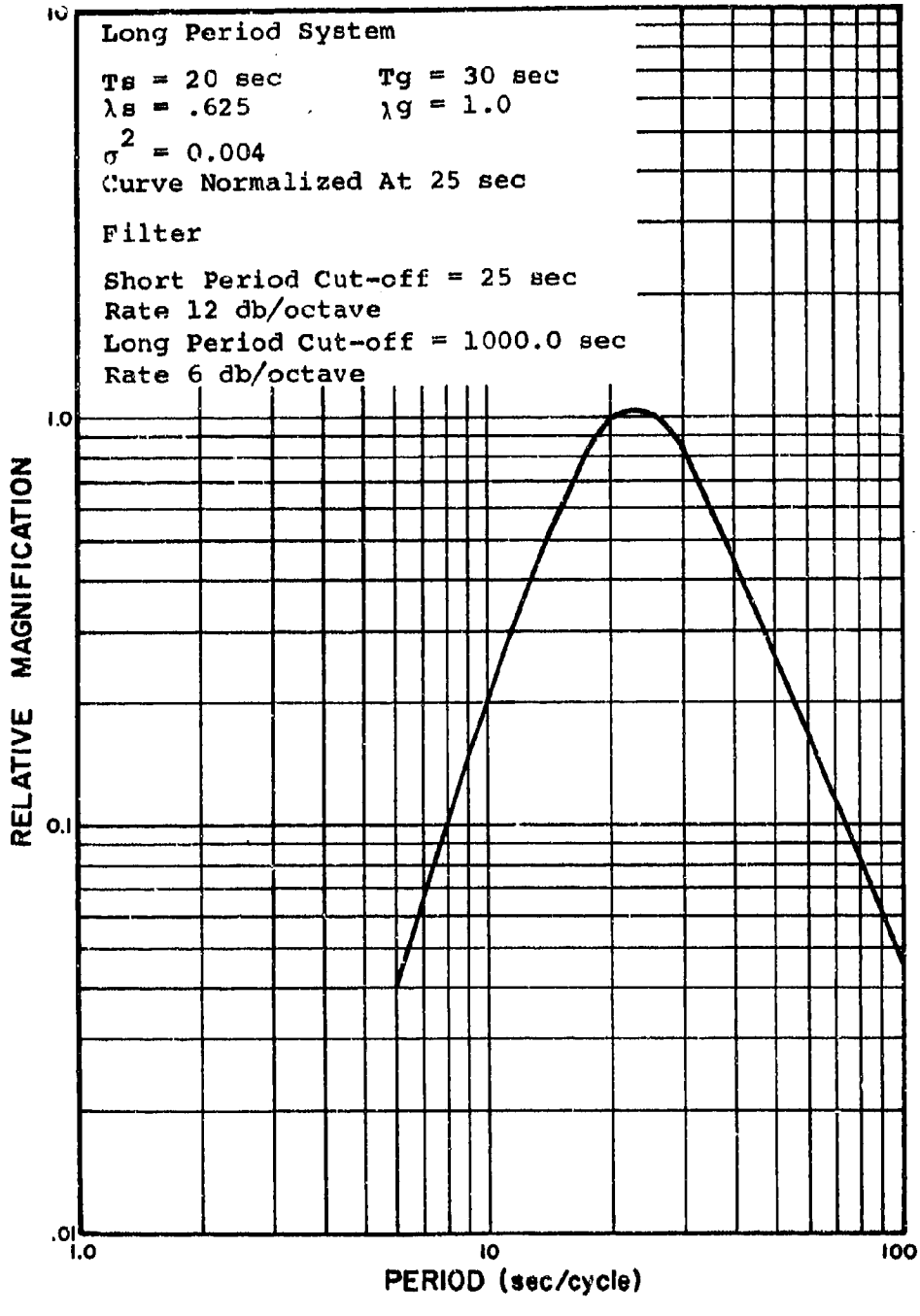

Figure 4. LRSM Long Period System Response

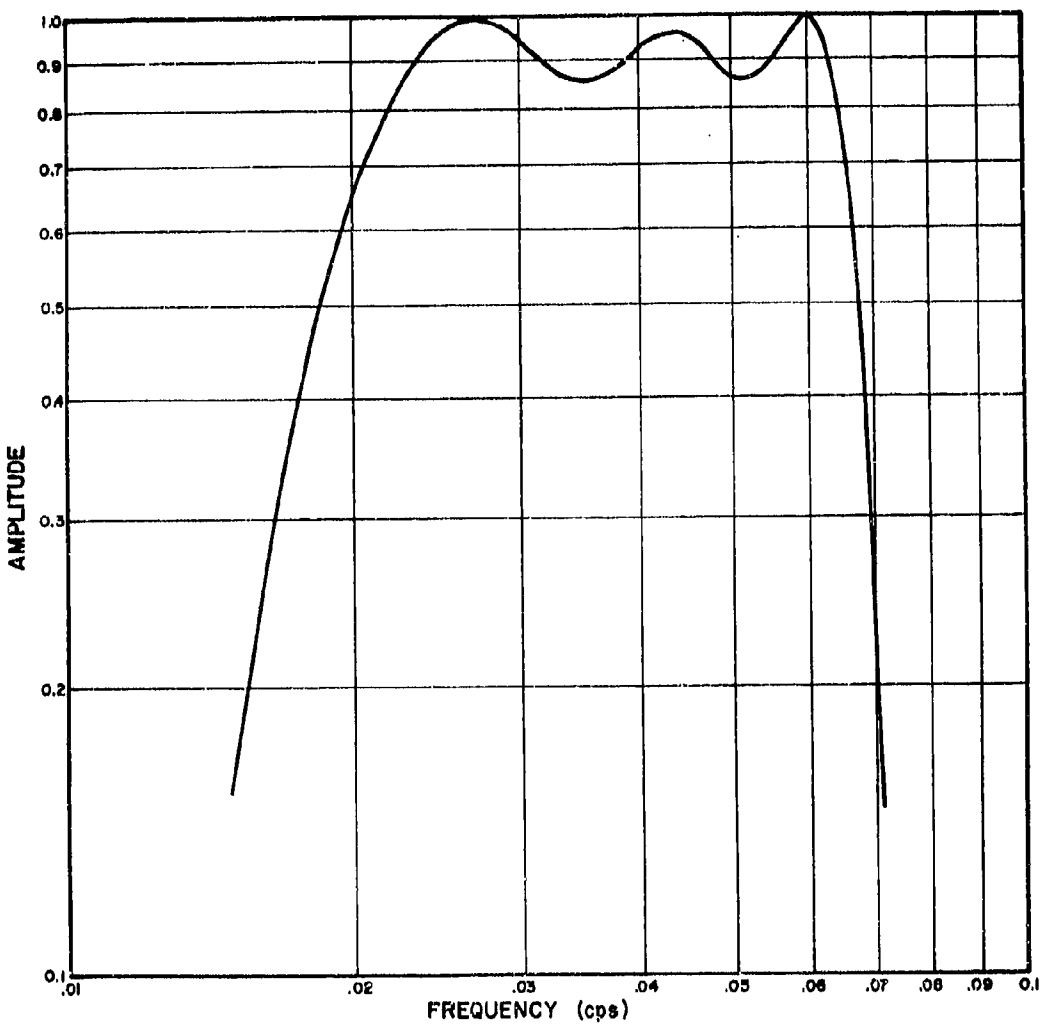

Figure 5. Digital Band-Pass Filter Response

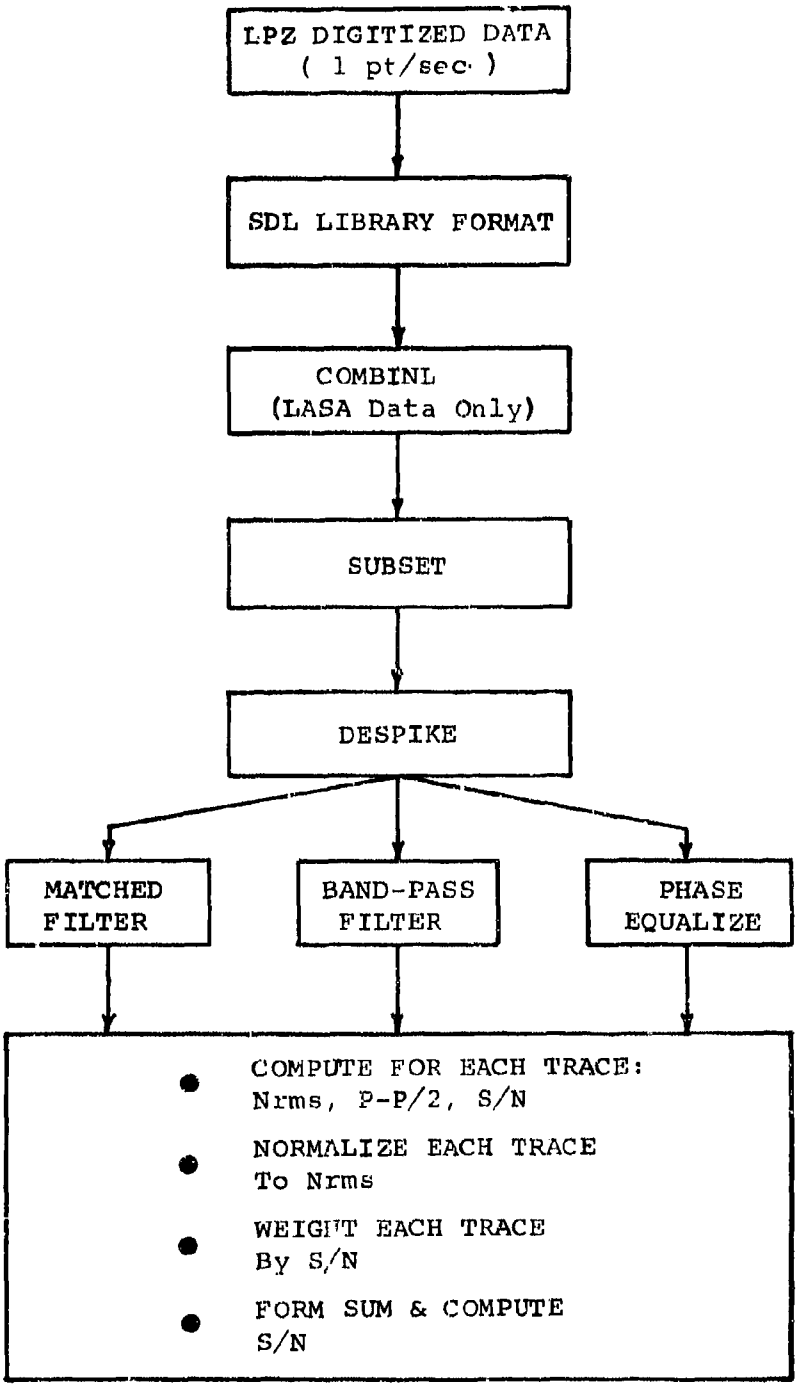

Figure 6. Data Processing Flow Chart

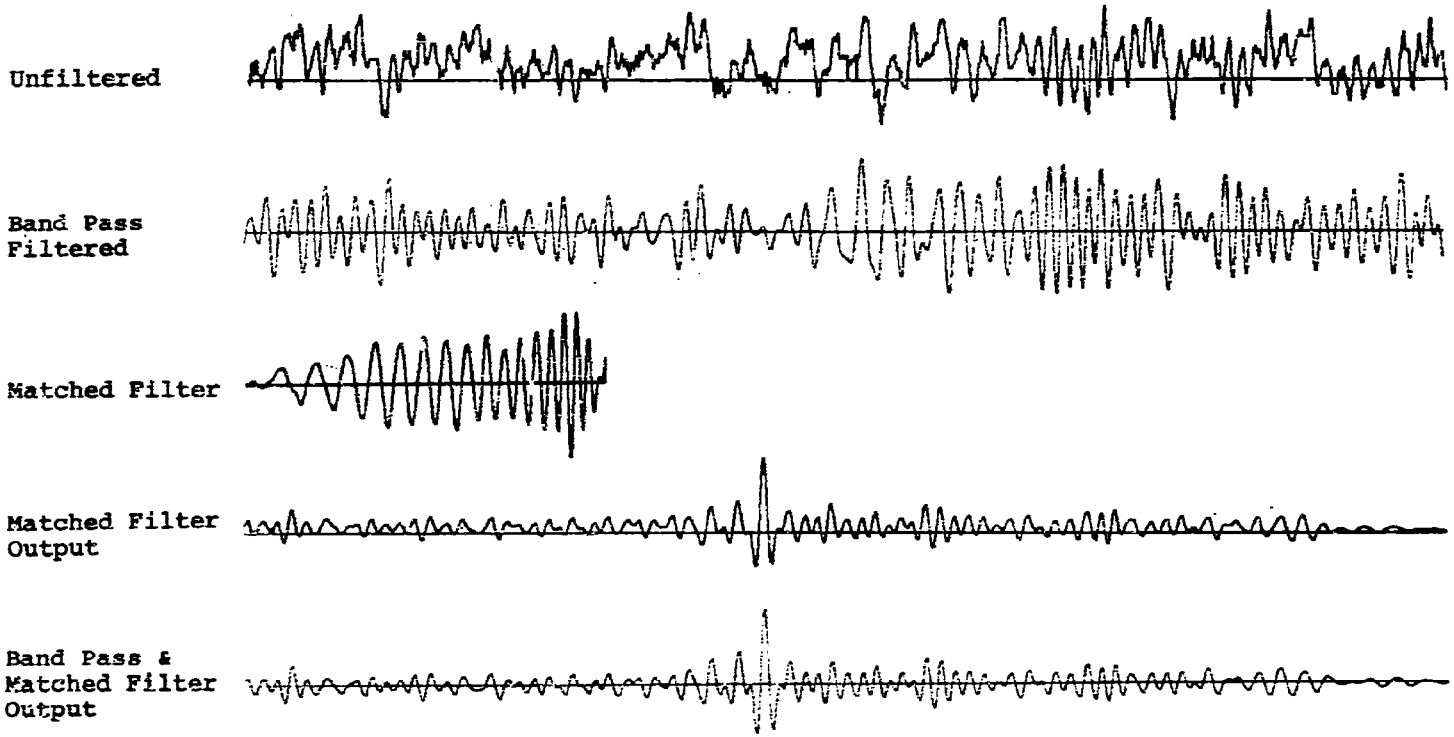

Figure 7. Comparison of Several Signal Enhancement Procedures For A Single LASA Element (B1 - LPZ)

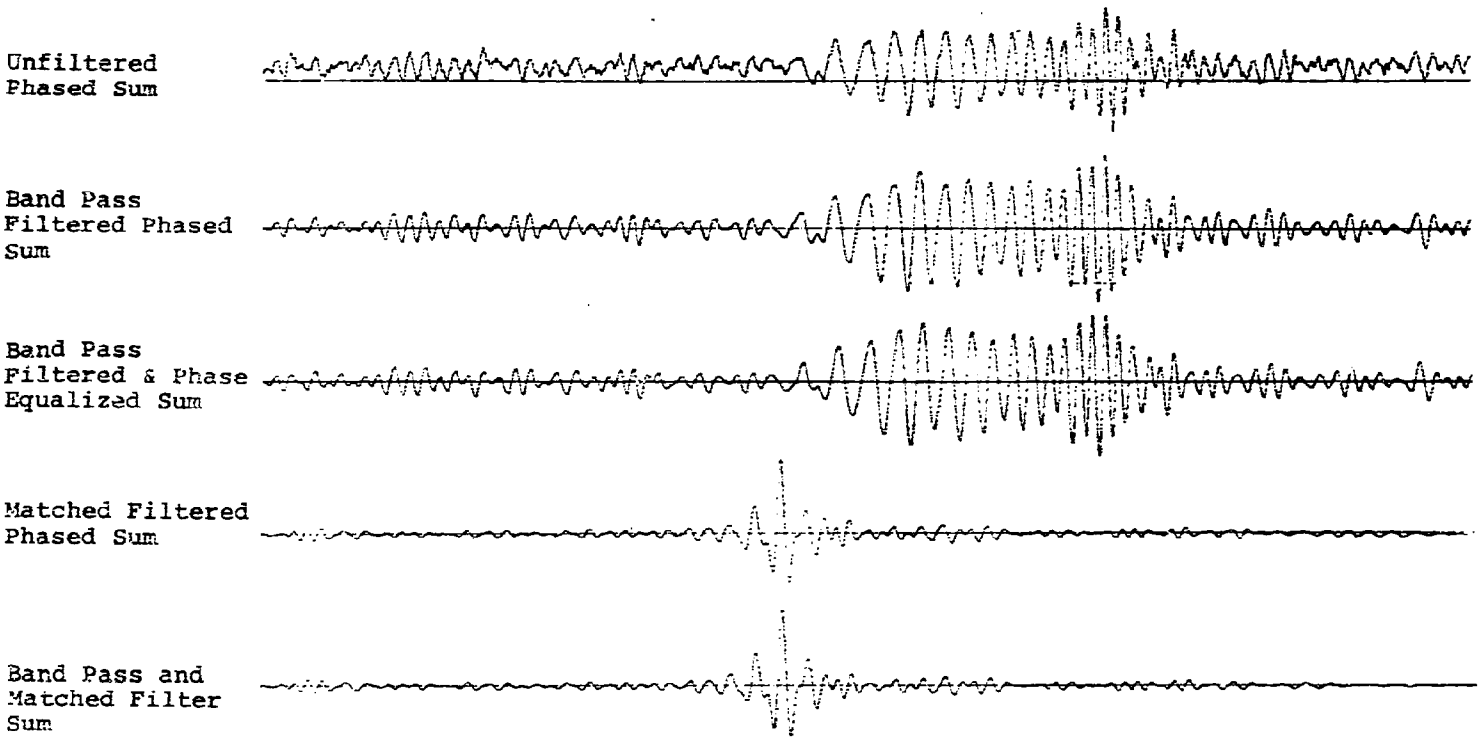

Figure 8. Comparison of Several Multichannel Signal Enhancement Procedures for 21 LASA LPZ Elements

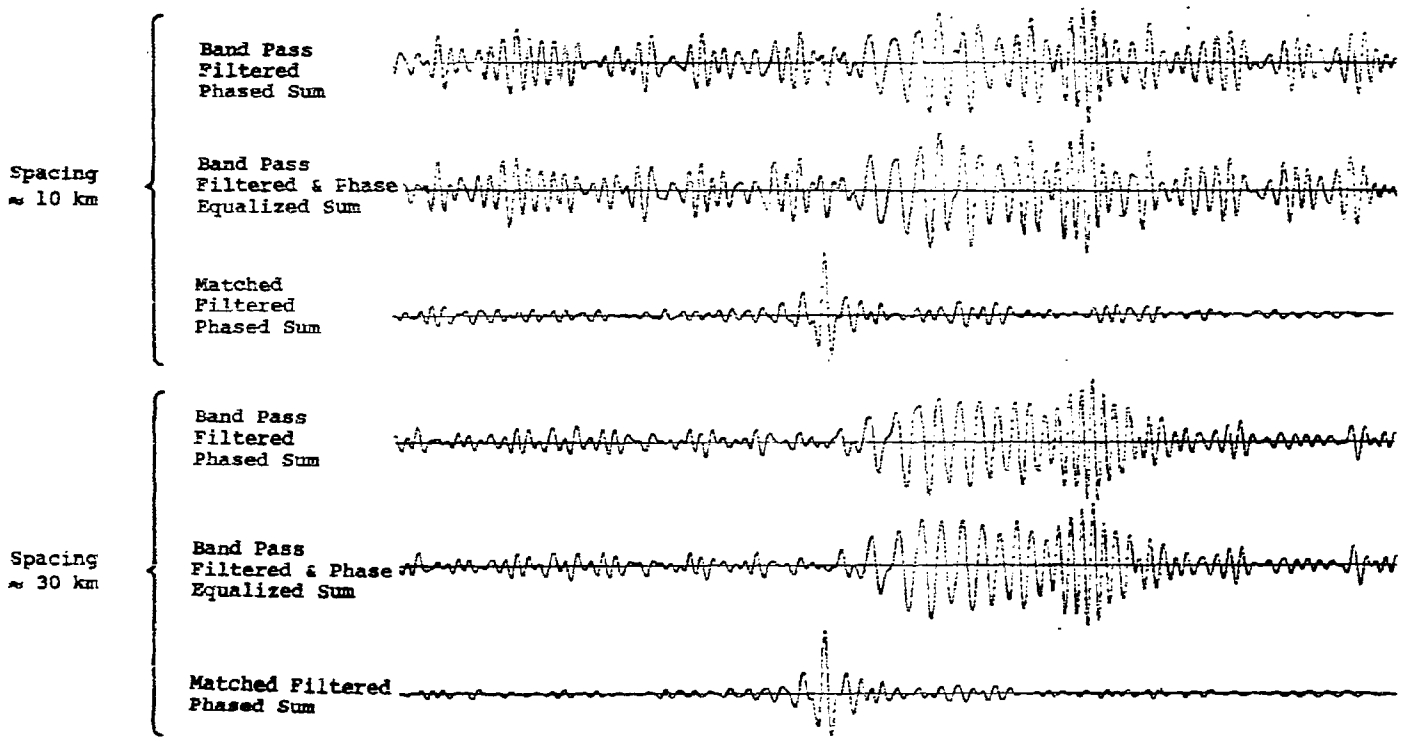

Figure 9. Typical Multi-Channel Combinations of 5 LASA LPZ Elements Showing the Effect of Inter-Sensor Spacing

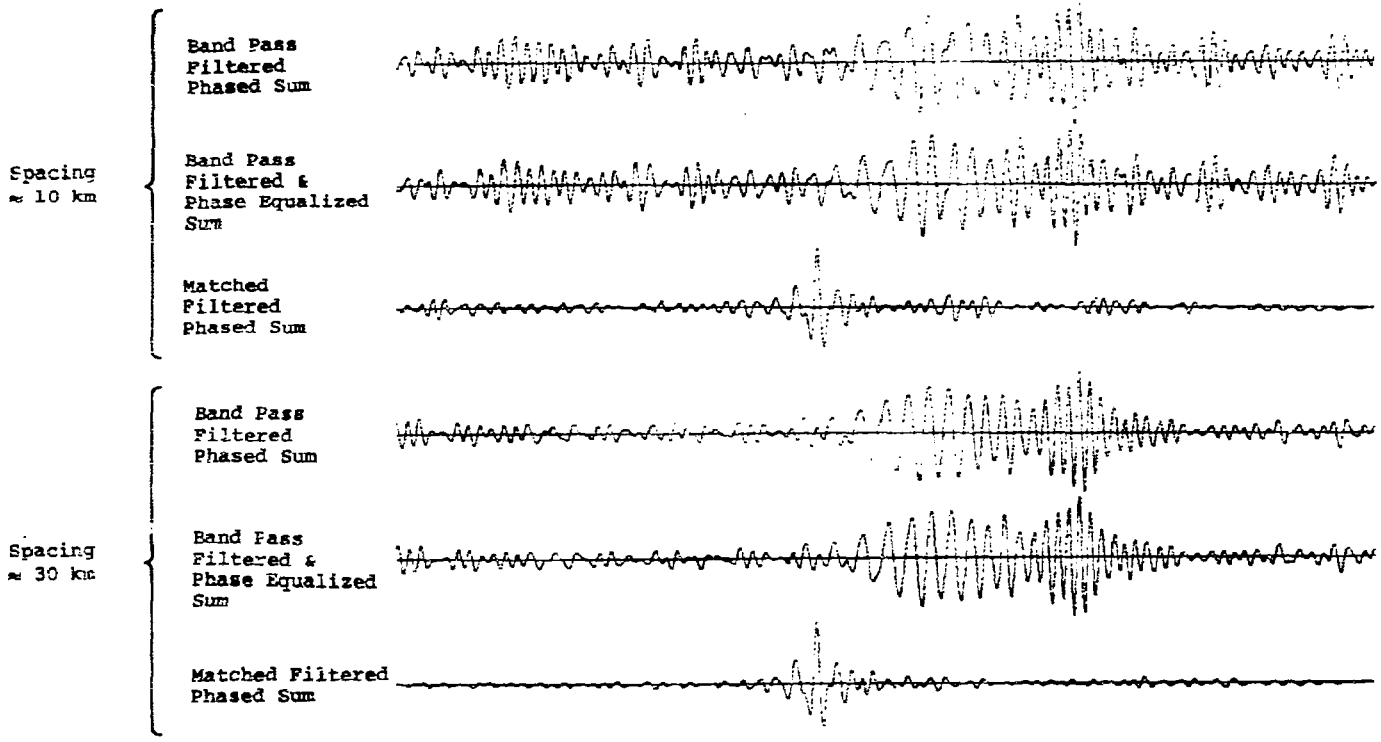

Figure 10. Typical Multi-Channel Combinations of 9 LASA LPZ Elements Showing the Effect of Inter-Sensor Spacing

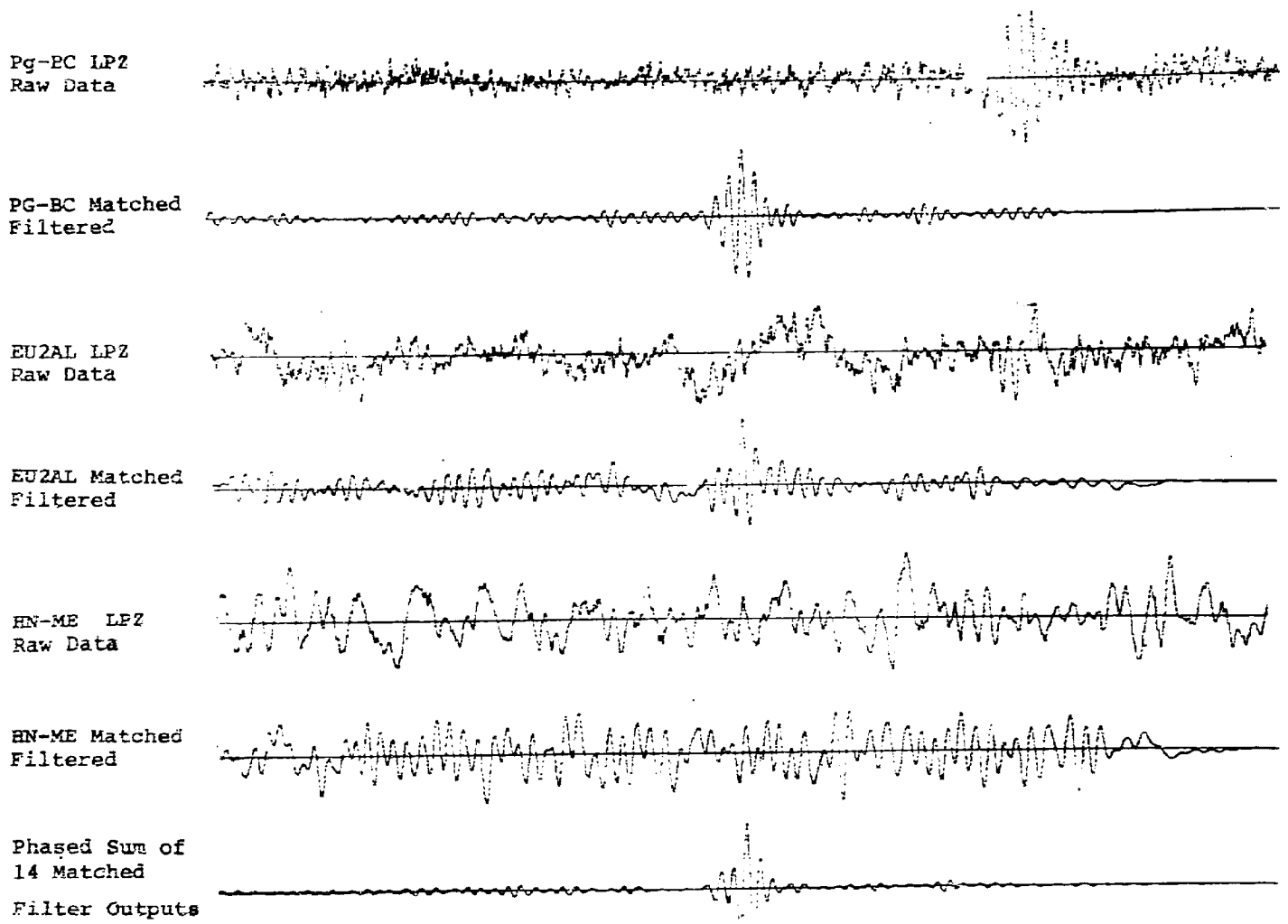

Figure 11. Typical Results of Matched Filter Processing of LRSM (& VELA Observatory) LPZ Seismograms, and the Sum of 14 Such Matched Filter Outputs.

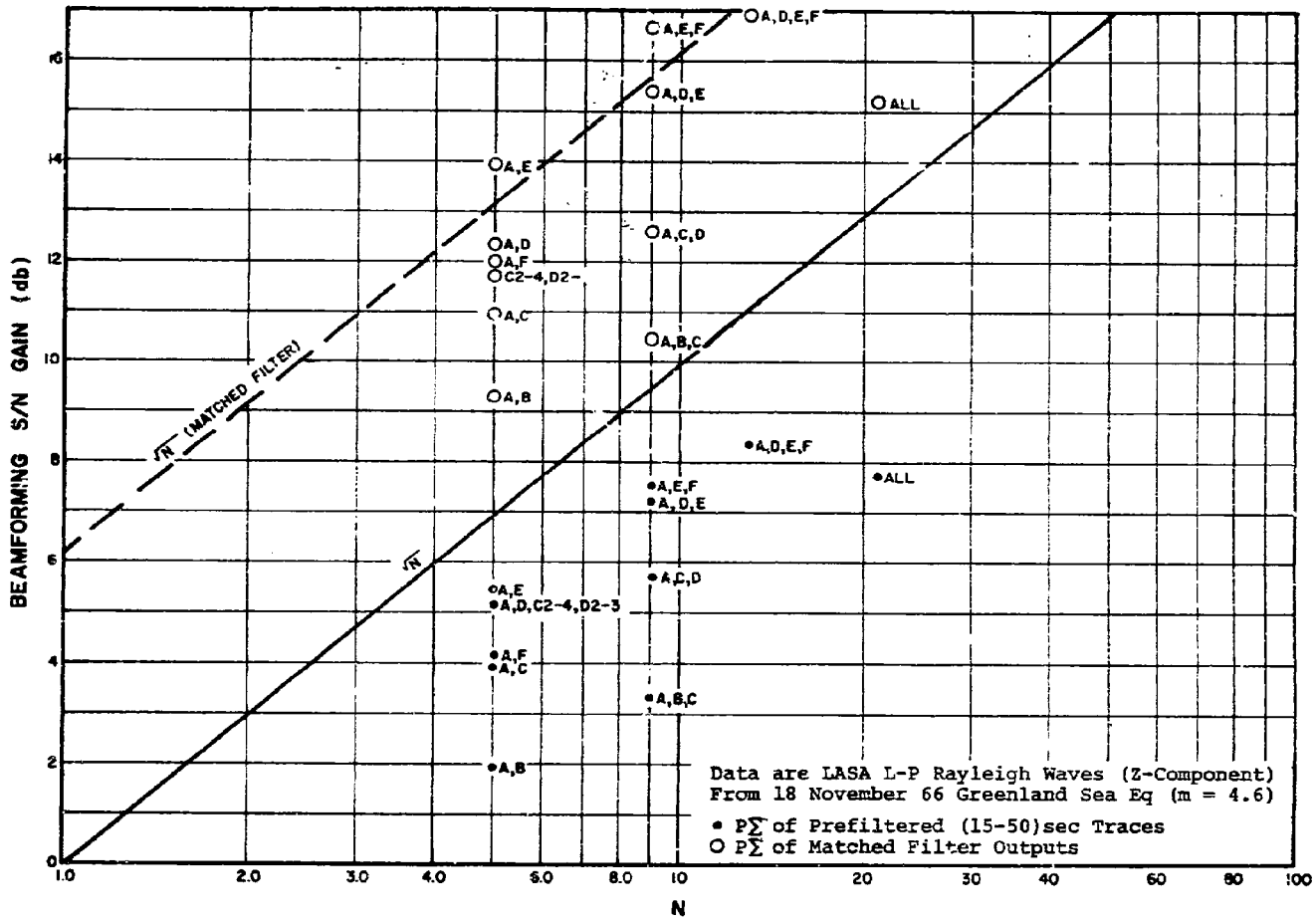

Figure 12. Rayleigh Wave Enhancement vs. Number of Sensors with Inter-Sensor Spacing as a Parameter

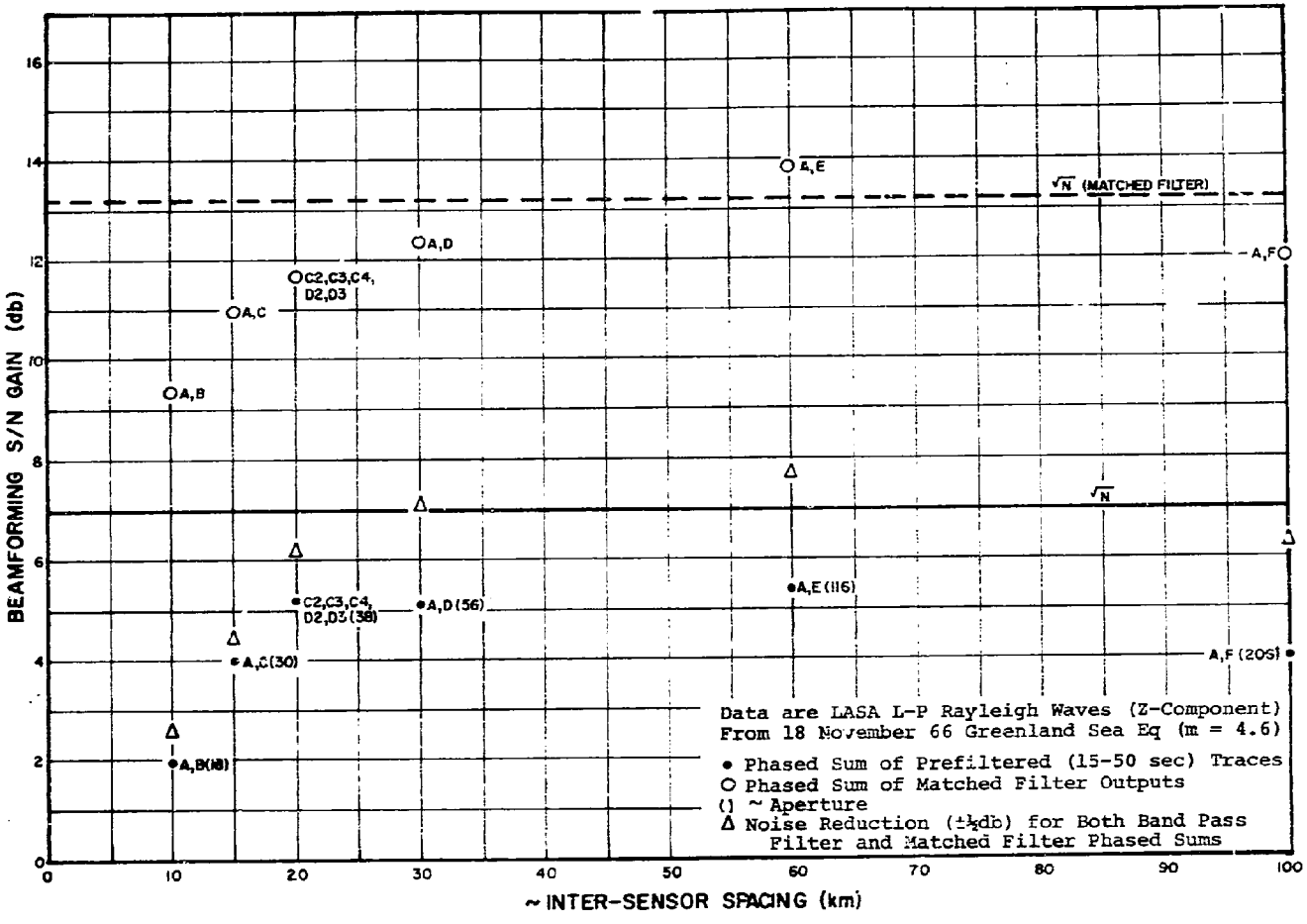

Figure 13. Rayleigh Wave Enhancement vs. Inter-Sensor Spacing (N=5)

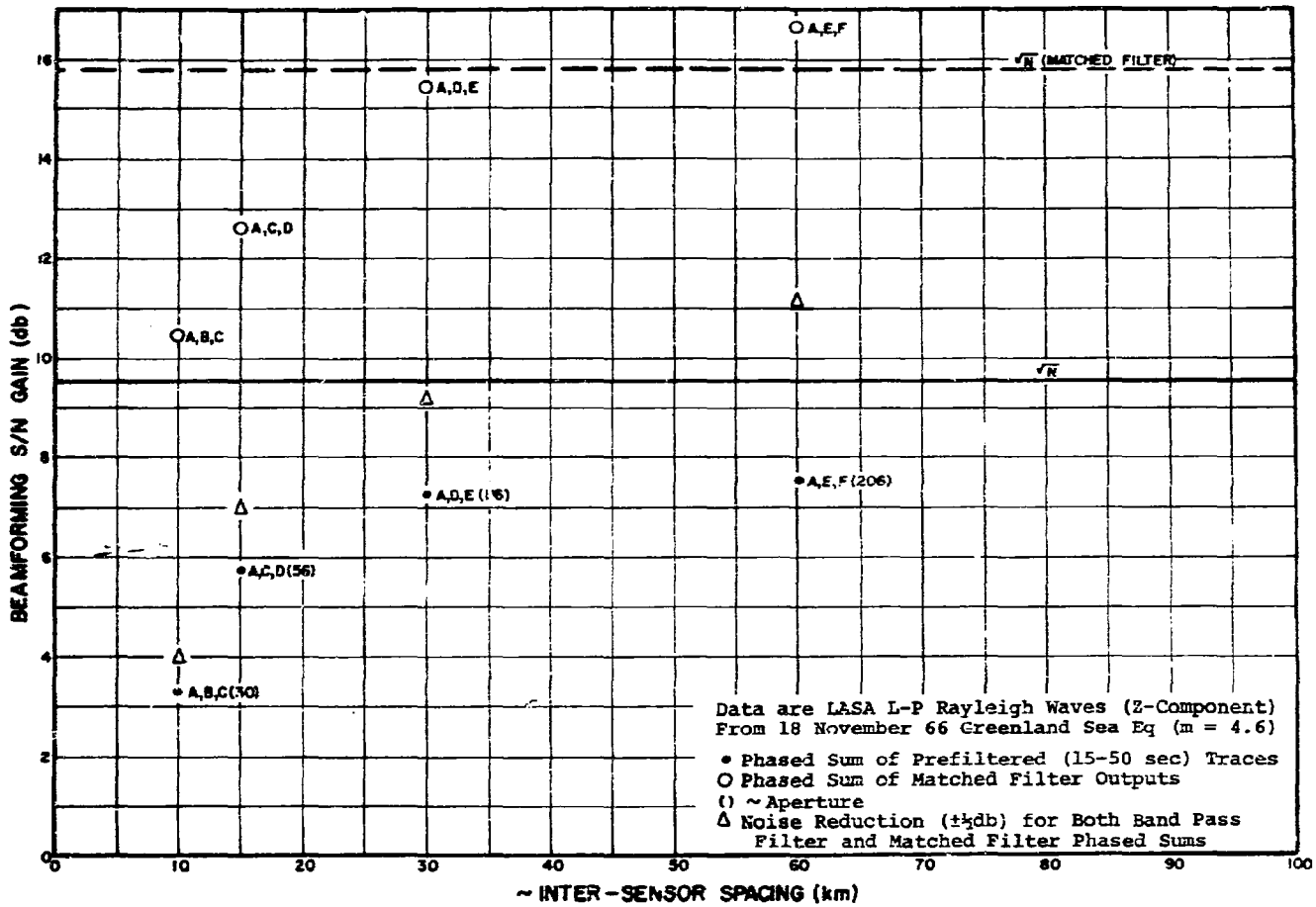

Figure 14. Rayleigh Wave Enhancement vs. Inter-Sensor Spacing (N=9)

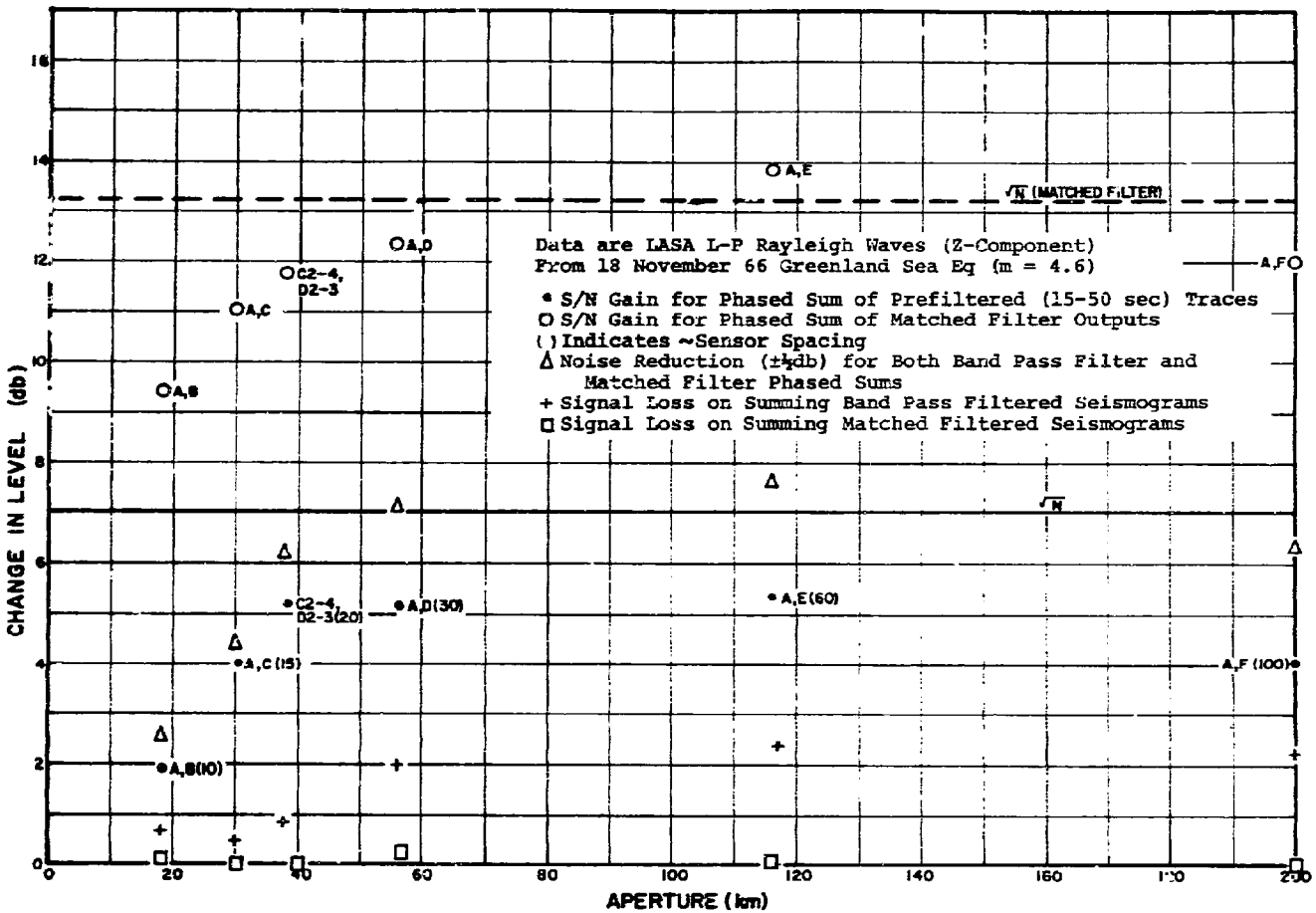

Figure 15. Rayleigh Wave Enhancement vs. Aperature (N=5)

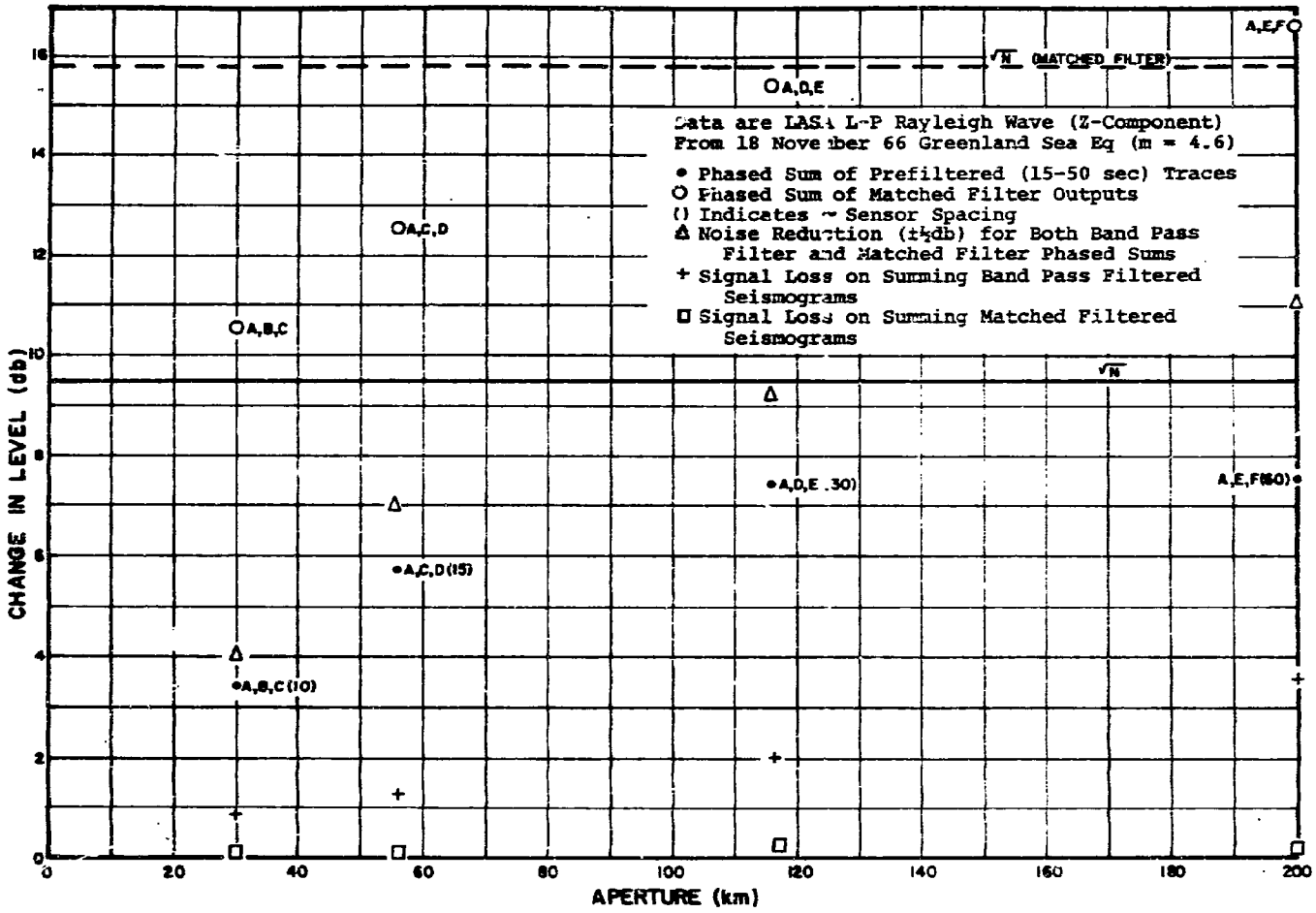

Figure 16. Rayleigh Wave Enhancement vs. Aperature (N=9)

Unclassified
Security Classification

DOCUMENT CONTROL DATA - R&D
(Security classification of title, body of abstract and indexing annotation must be entered when the overall report is classified)

1. ORIGINATING ACTIVITY *(Corporate author)*
TELEDYNE, INC.
ALEXANDRIA, VIRGINIA

2a. REPORT SECURITY CLASSIFICATION
Unclassified

2b. GROUP
---

3. REPORT TITLE
RAYLEIGH WAVE SIGNAL TO NOISE ENHANCEMENT FOR A SMALL TELESEISM USING LASA, LRSM, AND OBSERVATORY STATIONS

4. DESCRIPTIVE NOTES *(Type of report and inclusive dates)*
Scientific

5. AUTHOR(S) *(Last name, first name, initial)*
Alexander, S. S. and D. B. Rabenstine

6. REPORT DATE	7a. TOTAL NO. OF PAGES	7b. NO. OF REFS
21 August 1967	58	4

8a. CONTRACT OR GRANT NO.	9a. ORIGINATOR'S REPORT NUMBER(S)
F 33657-67-C-1313	194
b. PROJECT NO. VELA T/6702	
c. ARPA Order No. 624	9b. OTHER REPORT NO(S) *(Any other numbers that may be assigned this report)*
d. ARPA Program Code No. 5810	---

10. AVAILABILITY/LIMITATION NOTICES
This document is subject to special export controls and each transmittal to foreign governments or foreign national may be made only with approval of Chief, AFTAC.

11. SUPPLEMENTARY NOTES	12. SPONSORING MILITARY ACTIVITY
-----	ADVANCED RESEARCH PROJECTS AGENCY NUCLEAR TEST DETECTION OFFICE WASHINGTON, D. C.

13. ABSTRACT

Both single channel and array signal enhancement techniques have been applied to Rayleigh waves from a small Greenland Sea earthquake recorded at LASA and 13 LRSM or Observatory stations. Analysis of individual LASA long period recordings indicated that the matched filter increased S/N by more than 6 db over the mean S/N of band pass filtered (15-50 sec period) seismograms. Band pass filtering increased the mean S/N by only 1.5 db over the mean for unfiltered seismograms for LASA. Additional improvement in S/N from beam-forming both band passed and matched filtered traces approached the expected increase for uncorrelated noise provided the intersensor spacing (mesh-size) was at least 30 km. Comparable improvement was obtained for both single channel and beam-formed LRSM data. For LASA the beam-formed matched filter S/N for 13 stations was 17 db above the mean S/N for the individual band pass filtered seismograms; that for 13 LRSM stations was 15-16 db above the mean S/N of band pass filtered seismograms. Beam-forming matched filter seismograms consistently produced S/N values 7-9 db above the S/N for beam formed band pass filtered seismograms. The effects of such array parameters as number of sensors, sensor spacing, and aperture on signal enhancement are evaluated for this event.

DD FORM 1 JAN 64 1473

Unclassified
Security Classification

Unclassified
Security Classification

14 KEY WORDS	LINK A		LINK B		LINK C	
	ROLE	WT	ROLE	WT	ROLE	WT
LASA						
Matched Filter						
Seismic Noise						
Surface Wave Analysis						
Array Processing						

INSTRUCTIONS

1. ORIGINATING ACTIVITY: Enter the name and address of the contractor, subcontractor, grantee, Department of Defense activity or other organization *(corporate author)* issuing the report.

2a. REPORT SECURITY CLASSIFICATION: Enter the overall security classification of the report. Indicate whether "Restricted Data" is included. Marking is to be in accordance with appropriate security regulations.

2b. GROUP: Automatic downgrading is specified in DoD Directive 5200.10 and Armed Forces Industrial Manual. Enter the group number. Also, when applicable, show that optional markings have been used for Group 3 and Group 4 as authorized.

3. REPORT TITLE: Enter the complete report title in all capital letters. Titles in all cases should be unclassified. If a meaningful title cannot be selected without classification, show title classification in all capitals in parenthesis immediately following the title.

4. DESCRIPTIVE NOTES: If appropriate, enter the type of report, e.g., interim, progress, summary, annual, or final. Give the inclusive dates when a specific reporting period is covered.

5. AUTHOR(S): Enter the name(s) of author(s) as shown on or in the report. Enter last name, first name, middle initial. If military, show rank and branch of service. The name of the principal author is an absolute minimum requirement.

6. REPORT DATE: Enter the date of the report as day, month, year; or month, year. If more than one date appears on the report, use date of publication.

7a. TOTAL NUMBER OF PAGES: The total page count should follow normal pagination procedures, i.e., enter the number of pages containing information.

7b. NUMBER OF REFERENCES: Enter the total number of references cited in the report.

8a. CONTRACT OR GRANT NUMBER: If appropriate, enter the applicable number of the contract or grant under which the report was written.

8b, 8c, & 8d. PROJECT NUMBER: Enter the appropriate military department identification, such as project number, subproject number, system numbers, task number, etc.

9a. ORIGINATOR'S REPORT NUMBER(S): Enter the official report number by which the document will be identified and controlled by the originating activity. This number must be unique to this report.

9b. OTHER REPORT NUMBER(S): If the report has been assigned any other report numbers *(either by the originator or by the sponsor)*, also enter this number(s).

10. AVAILABILITY/LIMITATION NOTICES: Enter any limitations on further dissemination of the report, other than those imposed by security classification, using standard statements such as:

(1) "Qualified requesters may obtain copies of this report from DDC."

(2) "Foreign announcement and dissemination of this report by DDC is not authorized."

(3) "U. S. Government agencies may obtain copies of this report directly from DDC. Other qualified DDC users shall request through _____."

(4) "U. S. military agencies may obtain copies of this report directly from DDC. Other qualified users shall request through _____."

(5) "All distribution of this report is controlled. Qualified DDC users shall request through _____."

If the report has been furnished to the Office of Technical Services, Department of Commerce, for sale to the public, indicate this fact and enter the price, if known.

11. SUPPLEMENTARY NOTES: Use for additional explanatory notes.

12. SPONSORING MILITARY ACTIVITY: Enter the name of the departmental project office or laboratory sponsoring *(paying for)* the research and development. Include address.

13. ABSTRACT: Enter an abstract giving a brief and factual summary of the document indicative of the report, even though it may also appear elsewhere in the body of the technical report. If additional space is required, a continuation sheet shall be attached.

It is highly desirable that the abstract of classified reports be unclassified. Each paragraph of the abstract shall end with an indication of the military security classification of the information in the paragraph, represented as *(TS), (S), (C), or (U)*.

There is no limitation on the length of the abstract. However, the suggested length is from 150 to 225 words.

14. KEY WORDS: Key words are technically meaningful terms or short phrases that characterize a report and may be used as index entries for cataloging the report. Key words must be selected so that no security classification is required. Identifiers, such as equipment model designation, trade name, military project code name, geographic location, may be used as key words but will be followed by an indication of technical context. The assignment of links, rules, and weights is optional.

Unclassified
Security Classification